Development of a Novel CD4$^+$ TCR Transgenic Line That Reveals a Dominant Role for CD8$^+$ Dendritic Cells and CD40 Signaling in the Generation of Helper and CTL Responses to Blood-Stage Malaria

Daniel Fernandez-Ruiz,*,† Lei Shong Lau,* Nazanin Ghazanfari,*,† Claerwen M. Jones,* Wei Yi Ng,* Gayle M. Davey,* Dorothee Berthold,* Lauren Holz,*,† Yu Kato,* Matthias H. Enders,* Ganchimeg Bayarsaikhan,*,‡ Sanne H. Hendriks,* Lianne I. M. Lansink,§ Jessica A. Engel,§ Megan S. F. Soon,§ Kylie R. James,§ Anton Cozijnsen,¶ Vanessa Mollard,¶ Alessandro D. Uboldi,‖ Christopher J. Tonkin,‖ Tania F. de Koning-Ward,# Paul R. Gilson, Tsuneyasu Kaisho,†† Ashraful Haque,§ Brendan S. Crabb,** Francis R. Carbone,* Geoffrey I. McFadden,¶ and William R. Heath*,†**

We describe an MHC class II (I-A^b)–restricted TCR transgenic mouse line that produces CD4$^+$ T cells specific for *Plasmodium* species. This line, termed PbT-II, was derived from a CD4$^+$ T cell hybridoma generated to blood-stage *Plasmodium berghei* ANKA (PbA). PbT-II cells responded to all *Plasmodium* species and stages tested so far, including rodent (PbA, *P. berghei* NK65, *Plasmodium chabaudi* AS, and *Plasmodium yoelii* 17XNL) and human (*Plasmodium falciparum*) blood-stage parasites as well as irradiated PbA sporozoites. PbT-II cells can provide help for generation of Ab to *P. chabaudi* infection and can control this otherwise lethal infection in CD40L-deficient mice. PbT-II cells can also provide help for development of CD8$^+$ T cell–mediated experimental cerebral malaria (ECM) during PbA infection. Using PbT-II CD4$^+$ T cells and the previously described PbT-I CD8$^+$ T cells, we determined the dendritic cell (DC) subsets responsible for immunity to PbA blood-stage infection. CD8$^+$ DC (a subset of XCR1$^+$ DC) were the major APC responsible for activation of both T cell subsets, although other DC also contributed to CD4$^+$ T cell responses. Depletion of CD8$^+$ DC at the beginning of infection prevented ECM development and impaired both Th1 and follicular Th cell responses; in contrast, late depletion did not affect ECM. This study describes a novel and versatile tool for examining CD4$^+$ T cell immunity during malaria and provides evidence that CD4$^+$ T cell help, acting via CD40L signaling, can promote immunity or pathology to blood-stage malaria largely through Ag presentation by CD8$^+$ DC. ***The Journal of Immunology*****, 2017, 199: 4165–4179.**

Despite intervention strategies, malaria killed almost half a million people in 2015 (1). Murine models for malaria present similarities with human infections and allow for the detailed study of immunological processes of potential relevance to human disease (2–8). TCR transgenic murine lines specific for pathogen-derived Ags are powerful tools for studying the

*Department of Microbiology and Immunology, The Peter Doherty Institute for Infection and Immunity, The University of Melbourne, Parkville, Victoria 3000, Australia; †Australian Research Council Centre of Excellence in Advanced Molecular Imaging, The University of Melbourne, Parkville, Victoria 3010, Australia; ‡Division of Immunology, Department of Molecular Microbiology and Immunology, Graduate School of Biomedical Sciences, Nagasaki University, Nagasaki 852-8523, Japan; §Malaria Immunology Laboratory, QIMR Berghofer Medical Research Institute, Herston, Queensland 4006, Australia; ¶School of BioSciences, The University of Melbourne, Parkville, Victoria 3010, Australia; ‖Walter and Eliza Hall Institute of Medical Research, Parkville, Victoria 3052, Australia; #School of Medicine, Deakin University, Waurn Ponds, Victoria 3216, Australia; **Macfarlane Burnet Institute for Medical Research and Public Health, Melbourne, Victoria 3004, Australia; and ††Department of Immunology, Institute of Advanced Medicine, Wakayama Medical University, Wakayama 641-8509, Japan

ORCIDs: 0000-0002-4040-9121 (D.F.-R.); 0000-0001-8594-9554 (C.M.J.); 0000-0002-7027-8783 (W.Y.N.); 0000-0002-9514-6023 (G.M.D.); 0000-0002-9045-6348 (D.B.); 0000-0003-4897-0981 (L.H.); 0000-0003-3567-3726 (G.B.); 0000-0003-1965-1287 (L.I.M.L.); 0000-0001-8563-849X (M.S.F.S.); 0000-0002-7107-0650 (K.R.J.); 0000-0001-9222-8229 (V.M.); 0000-0001-5810-8063 (T.F.d.K.-W.); 0000-0003-2616-1665 (T.K.); 0000-0003-2260-0026 (A.H.); 0000-0002-5351-1627 (G.I.M.); 0000-0001-9670-259X (W.R.H.).

Received for publication February 7, 2017. Accepted for publication October 5, 2017.

This work was supported by the National Health and Medical Research Council of Australia and the Australian Research Council.

D.F.-R. designed and performed the research and wrote the manuscript; L.S.L., N.G., C.M.J., W.Y.N., G.M.D., D.B., L.H., Y.K., G.B., S.H.H., K.R.J., M.H.E., L.I.M.L., J.A.E., and M.S.F.S. performed research; A.C., V.M., T.F.d.K.-W., P.R.G., A.D.U., C.J.T., T.K., and G.I.M. provided reagents; A.H., B.S.C., and F.R.C. designed the research; W.R.H. designed the research and wrote the manuscript.

Address correspondence and reprint requests to Prof. William R. Heath, The University of Melbourne, The Peter Doherty Institute, 792 Elizabeth Street, Parkville, VIC 3000, Australia. E-mail address: wrheath@unimelb.edu.au

The online version of this article contains supplemental material.

Abbreviations used in this article: B6, C57BL/6; cDC, conventional DC; CTV, CellTrace Violet; DC, dendritic cell; DN, double-negative; DT, diphtheria toxin; ECM, experimental cerebral malaria; HFF, human foreskin fibroblast; iLN, inguinal LN; iRBC, infected RBC; IRF, IFN regulatory factor; KO, knockout; LN, lymph node; MHC I, MHC class I; MHC II, MHC class II; PbA, *Plasmodium berghei* ANKA; poly(I:C), polyinosinic-polycytidylic acid; RAS, radiation-attenuated sporozoite; ROR, retinoic acid–related orphan receptor; Tfh, follicular Th; uGFP, ubiquitously expressed GFP; WT, wild-type.

mechanisms involved in the development of immune responses during infection. Their ease of use and potential for manipulation offer a much broader range of opportunities for the study of T cell responses than are feasible using the endogenous T cell repertoire.

The lack of TCR transgenic mouse lines specific for *Plasmodium* Ags led to the generation of transgenic malaria parasites expressing model Ags, such as PbTG and OVA–*Plasmodium berghei* ANKA (PbA) (2, 4, 9, 10), for which widely used murine T cell lines such as OT-I and OT-II could be used to monitor specific T cell responses. Although the use of these parasites in conjunction with model T cell lines has aided the study of antimalarial $CD4^+$ and $CD8^+$ T cell responses (6, 11–15), wild-type (WT) parasites and transgenic T cells capable of recognizing authentic parasite-derived Ags are preferred, as they more closely resemble endogenous responses to natural infections. With this in mind, we recently generated a murine TCR transgenic line of PbA-specific $CD8^+$ T cells, termed PbT-I (8, 16). In this study, we describe an MHC class II (MHC II)–restricted ($I\text{-}A^b$) TCR murine line, termed PbT-II, that responds to a parasite Ag expressed across multiple rodent and human *Plasmodium* species, making it a general tool for studying malaria immunity in C57BL/6 (B6) mice. PbT-II TCR transgenic mice add to the existing $I\text{-}E^d$–restricted B5 TCR transgenic mice (2, 4, 17) to extend the set of available tools for the analysis of $CD4^+$ T cell responses to parasites during *Plasmodium* infection of B6 mice.

$CD4^+$ T cells orchestrate both humoral and cellular adaptive immune responses against pathogens. Cross-talk between $CD4^+$ T cells and naive B cells resulting in Ig class switching is essential for the clearance of certain pathogens such as *Plasmodium chabaudi* AS. Thus, mice lacking $CD4^+$ T cells or B cells are unable to control parasitemia in this model (17). Another important role for $CD4^+$ T cells is the provision of help resulting in the licensing of dendritic cells (DC) for the effective priming of $CD8^+$ T cells. However, although $CD4^+$ T cell help is essential for primary responses to certain pathogens, such as HSV (11, 18), it is dispensable during infection with influenza A virus, lymphocytic choriomeningitis virus, or *Listeria monocytogenes* (14, 19–21). It is understood that in the latter cases, sufficient engagement of receptors for pathogen-associated molecular patterns on DC by material derived from the infectious agent (6, 22), or cytokines secreted by innate cells upon recognition of the pathogen (23, 24), bypasses the need for $CD4^+$ T cell help. In the case of PbA infection, the helper dependence of $CD8^+$ T cell responses has not been directly addressed. PbA infection of B6 mice leads to the development of experimental cerebral malaria (ECM), a pathology mediated by $CD8^+$ T cells that is used as a model for human cerebral malaria (25). Therefore, dissection of the mechanisms that lead to $CD8^+$ T cell activation in this model is of importance to better understand this pathology. ECM was abolished when $CD4^+$ T cells were depleted during the early stages of the infection in a number of studies (26–30), suggesting that $CD8^+$ T cell priming relies on $CD4^+$ T cell help. Indeed, depletion of $CD4^+$ T cells during infection with the transgenic malaria parasite PbTG resulted in diminished OT-I cell proliferation (31). However, transfer of OT-I cells into PbTG-infected $RAG1^{-/-}$ mice, lacking T cells, resulted in the development of ECM in the absence of $CD4^+$ T cells (9). The role of $CD4^+$ T cells in activating DC for priming CTL responses during blood-stage PbA infection therefore remained to be conclusively defined.

DC are effective APC that prime T cells for the generation of pathogen-specific adaptive immune responses. The DC compartment is comprised of a heterogeneous array of cell subsets with marked functional specialization (32). Determining the relative contribution of DC subsets to T cell priming is of great importance, especially for the development of new generations of vaccines in which Ag is delivered to a specific DC subset seeking induction of optimal T cell responses. $CD8^+$ DC possess specialized machinery to perform Ag cross-presentation to $CD8^+$ T cells, which other conventional DC (cDC) lack (33, 34). However, both $CD8^+$ and $CD8^-$ DC are capable of Ag presentation to $CD4^+$ T cells via MHC II (35, 36). Consistent with these observations, $CD8^+$ DC from mice infected with PbTG were significantly more effective than $CD8^-$ DC at presenting OVA Ag to $CD8^+$ T cells in vitro, whereas both DC subsets were capable of priming $CD4^+$ T cells (9). Also, depletion of $CD8^+$ DC in PbA-infected mice resulted in a sharp decrease in the numbers of activated endogenous $CD8^+$ T cells in the spleen, and $CD4^+$ T cell activation was also impaired (37). A similar result was obtained when $CD8^+$ DC were depleted in *P. chabaudi*–infected mice (38). Another study analyzing $CD4^+$ T cell responses to *P. chabaudi* Ag showed $CD8^+$ DC as superior to $CD8^-$ DC at MHC II presentation in the steady-state, but the latter were more efficient during infection (39). In the *P. chabaudi* model, mice devoid of $CD8^+$ DC developed higher peaks of parasitemia and more pronounced relapses than did their WT counterparts (40). These results suggested an important role for $CD8^+$ DC in the development of T cell responses against blood-stage malaria parasites.

In this study, we introduce a $CD4^+$ T cell transgenic mouse line specific for a malaria parasite Ag, termed PbT-II, that is cross-reactive with a broad range of malaria parasites, including PbA, *P. chabaudi*, and *Plasmodium yoelii*, and even the human parasite *Plasmodium falciparum*. These cells are also cross-reactive, albeit weakly, to PbA sporozoites. Therefore, PbT-II cells are broadly applicable for the study of $CD4^+$ T cell function in multiple malaria models.

Materials and Methods

Ethics statement

All procedures were performed in strict accordance with the recommendations of the Australian code of practice for the care and use of animals for scientific purposes. The protocols were approved by the Biochemistry and Molecular Biology, Dental Science, Medicine (Royal Melbourne Hospital), Microbiology and Immunology, and Surgery (Royal Melbourne Hospital) Animal Ethics Committee, The University of Melbourne (ethic project IDs 0810527, 0811055, 0911527, 1112347, and 1513505).

Mice, mosquitos, and parasites

B6, BALB/c, MHC class I $(\text{MHC I})^{-/-}$ (41), $IAE^{-/-}$ (MHC II–deficient) (42), $RAG1^{-/-}$ (43), $Batf3^{-/-}$ (44), IFN regulatory factor $(IRF8)^{-/-}$ (45), XCR1-DTRvenus (46), CD11cDTR (47), $CD40^{-/-}$ (48), and $CD40L^{-/-}$ (49) mice and the transgenic strains OT-II (50), gDT-II (51), PbT-I (16), and PbT-II were used between 6 and 12 wk and were bred and maintained at the Department of Microbiology and Immunology, The Peter Doherty Institute. $Batf3^{-/-}$ mice, provided by K.M. Murphy (Washington University), were backcrossed 10 generations to B6 for use in this study. Transgenic T cell lines were crossed to mice ubiquitously expressing GFP (uGFP) or with CD45.1 (Ly5.1) mice to allow for the differentiation of these cells from endogenous T cells after adoptive transfer into recipient Ly5.2 B6 mice. XCR1-DTRvenus and CD11cDTR mice were treated with diphtheria toxin (DT; Calbiochem) as indicated in the figure legends. Animals used for the generation of the sporozoites were 4- to 5-wk-old male Swiss Webster mice purchased from Monash Animal Services (Melbourne, VIC, Australia) and maintained at the School of Botany, The University of Melbourne (Melbourne, VIC, Australia).

Anopheles stephensi mosquitoes (strain STE2/MRA-128 from the Malaria Research and Reference Reagent Resource Center) were reared and infected with PbA as described (52). Sporozoites were dissected from mosquito salivary glands, resuspended in cold PBS, and irradiated with 2×10^4 rad using a gamma ^{60}Co source. Radiation-attenuated sporozoites (RAS; 5×10^4) in 0.2 ml of PBS were i.v. administered to recipient mice.

The rodent malaria lines PbA clone 15cy1, *P. berghei* NK65, *P. chabaudi* AS, and *P. yoelii* 17XNL were used in this study. Unless otherwise stated,

mice were infected i.v. with 10^4 PbA, *P. berghei* NK65, *P. chabaudi*, or *P. yoelii* 17XNL infected RBC (iRBC) in 0.2 ml of PBS.

The *P. falciparum* 3D7 strain was cultured in human erythrocytes (Australian Red Cross Blood Bank, blood group O^+) at 4% hematocrit in AlbuMAX II media (RPMI 1640–HEPES, 0.5% AlbuMAX II [Life Technologies], 0.2% $NaHCO_3$) at 37°C as described previously (53). Synchronous schizont-stage parasites were isolated from uninfected erythrocytes by passage through a magnetized column (Miltenyi Biotec) in PBS. The parasites were pelleted by centrifugation and stored at −80°C.

Toxoplasma gondii tachyzoites (Pru strain) were maintained in human foreskin fibroblasts (HFFs) in D1 medium (DMEM supplemented with 1% FCS [Invitrogen] and 2 mM GlutaMAX [Life Technologies]) in a humidified atmosphere of 10% CO_2 at 37°C. Prior to inoculation with parasites, HFFs were maintained in D10 medium (DMEM supplemented with 10% Cosmic Calf serum [Thermo Scientific] and 2 mM GlutaMAX). Freshly egressed tachyzoites from a T25 flask (Corning) were passed through a 27-gauge needle to ensure complete release from HFFs, before centrifuging at 450 rpm for 5 min at room temperature to pellet host cell debris. The supernatant was centrifuged at 2000 rpm for 5 min to pellet parasites. The parasites were washed twice with 10 ml Dulbecco's PBS. As a control for host cell factors, a monolayer of HFFs grown in a T25 flask (1×10^6 cells) was scraped and passed through a 27-gauge needle, followed by a 30-gauge needle, to completely lyse the HFFs. The HFF membranes were pelleted by centrifugation at 2000 rpm for 5 min and washed twice with PBS.

Generation of transgenic PbT-II mice

Transgenic PbT-II mice were generated using the V(D)J segments of the TCRα and TCRβ genes of a $CD4^+$ T cell hybridoma (termed D78) specific for an unidentified blood-stage PbA Ag. This hybridoma was derived from T cells extracted from the spleen of a B6 mouse at day 7 postinfection with PbA. Splenocytes (3×10^6) from a mouse previously infected with PbA were cocultured with 5×10^5 cDC (extracted from the spleen of Flt3 ligand–treated B6 mice) that were preloaded for 2 h with 2×10^6 PbA schizont lysate as previously described (54) in complete RPMI 1640 at 6.5% CO_2, 37°C. One week later, cultured cells were restimulated for a week with fresh DC and PbA schizont lysate. To generate PbA-specific hybridomas, in vitro–cultured cells were then fused with the BWZ36.GFP fusion partner and exposed to drug selection (55). This led to isolation of the I-A^b–restricted D78 hybridoma from which PbT-II TCR genes were derived. Vα and Vβ usage by D78 was defined by FACS staining with a panel of Vα TCR Abs and the mouse Vβ TCR screening panel (BD Biosciences).

The TCR α region was amplified by PCR from the cDNA of the D78 hybridoma using the forward primer 5′-GGATCCAGGAATGGACAAGATTCTG-3′ containing a BamHI recognition sequence at the 5′ end, designed to bind the 5′ untranslated region of Vα2, and the reverse primer 5′-CAGATCTCAACTGGACCACAG-3′ containing a BglII recognition sequence at the 5′ end, specific for the Cα region. Sequencing analysis revealed that the TCR α-chain consisted of Vα2.7, Jα12, and Cα gene segments. The Vα2.7-Jα12-Cα segment was cloned into the BamHI site of the pES4 cDNA expression vector (56).

TCR Vβ usage was confirmed by PCR on cDNA converted from the RNA of the D78 hybridoma using the primer 5′-GAAGATGGTGGGGCTTTCAAGGATC-3′, specific for the Vβ12 gene. Sequencing analysis revealed that the TCR β-chain consisted of Vβ12, Dβ2, and Jβ2.4. The TCR β-chain VDJ segment was amplified by PCR from the genomic DNA of the D78 hybridoma using the forward primer 5′-GGATCGATCACACTTGTTTTCCGTG-3′ specific for Vβ12, incorporating a ClaI restriction enzyme site at the 5′ end, and the reverse primer 5′-GATCGATCAGCTCACCTAACACGAGGA-3′ specific for Jβ2.4 and incorporating a ClaI site at the 5′ end and sequenced. The Vβ12-Dβ2-Jβ2.4 segment was found to contain a ClaI within its sequence, so a new segment was synthetized in which the ClaI site (5′-ATCGAT-3′, coding for the amino acids Asp and Arg) was changed for 5′-ATCGAC-3′ (no change in amino acid sequence). The new segment was cloned into the unique ClaI restriction site of the p3A9CβTCR genomic expression vector (50).

The α- and β-chain vector sequences were removed using combined ClaI/NotI and ApaI/NotI restriction enzyme digests, respectively, and coinjected into blastocysts of B6 mice to generate transgenic founder mice.

DC isolation

DCs were purified from the spleens of mice as previously described (9). Briefly, spleens were finely minced and digested in 1 mg/ml collagenase 3 (Worthington Biochemical) and 20 μg/ml DNase I (Roche) under intermittent agitation for 20 min at room temperature. DC–T cell complexes were then disrupted by adding EDTA (pH 7.2) to the digest to a final concentration of 7.9 mM and continuing the incubation for 5 min. After removing undigested fragments by filtering through a 70-μm mesh, cells were resuspended in 5 ml of 1.077 g/cm^3 isosmotic Nycodenz medium (Nycomed Pharma, Oslo, Norway), layered over 5 ml of Nycodenz medium and centrifuged at $1700 \times g$ at 4°C for 12 min. In the experiments to determine MHC restriction by the hybridomas, the light density fraction was collected and DC were negatively enriched by incubation with a mixture of rat monoclonal anti-CD3 (clone KT3-1.1), anti–Thy-1 (clone T24/31.7), anti-Gr1 (clone RB68C5), anti-CD45R (clone RA36B2), and anti-erythrocyte (clone TER119) Abs followed by immunomagnetic bead depletion using BioMag goat anti-rat IgG beads (Qiagen).

In the experiments involving analyses of DC subsets, cells obtained after centrifugation in Nycodenz medium were stained for CD11c, MHC II, CD8, and CD4 and sorted into (MHC $II^{hi}CD11c^{hi}$) $CD8^+CD4^-$ ($CD8^+$ DC), $CD8^-CD4^+$ ($CD4^+$ DC), or $CD8^-CD4^-$ (double-negative [DN] DC) using a FACSAria III sorter (BD Biosciences).

DC were resuspended in complete DMEM medium supplemented with 10% FCS before use in functional assays.

Functional assay with hybridomas and IL-2 ELISA

For in vitro stimulation assays, DC (5×10^4 per well) were cultured for 1 h with titrated amounts of lysed whole blood containing mixed stages of PbA parasites before adding 5×10^4 D78 or PbA-specific MHC I–restricted B4 hybridoma cells (16). For ex vivo experiments, DC were extracted from the spleens of PbA-infected mice on day 3 postinfection with 10^6 iRBC.

After culture for 40 h at 37°C in 6.5% CO_2, supernatants were collected and concentrations of IL-2 were assessed using the mouse IL-2 ELISA Ready-SET-Go! kit (eBioscience) following the manufacturer's instructions. Data were represented using logarithmic scales. Because it would not be possible to represent concentration values of 0 in logarithmic scales, all data values were increased by 1. The detection limit of the mouse IL-2 ELISA Ready-SET-Go! kit is 2 pg/ml.

The calculation of the net contribution of DC subsets to MHC II presentation was done by multiplying the mean IL-2 values induced by $CD4^+$, $CD8^+$, or DN DC in Fig. 5B by the relative abundance of the corresponding DC subset in the spleen (in our experiments, MHC $II^{hi}CD11c^{hi}$ cells in the spleen contained 55.1% $CD4^+$ DC, 13.4% DN DC, and 17.7% $CD8^+$ DC on average). The numbers obtained from all three DC subsets, representing the IL-2 stimulation corrected to relative DC abundance, were added and the percentage of each individual DC subset in the total number obtained was calculated. This was done for all five DC numbers tested in Fig. 5B (3.125×10^3 to 50×10^3 DC per well) and the average of the five values obtained for each DC subset was calculated.

RBC coating

Blood was collected from a naive B6 donor. After estimating the concentration of RBC, blood was washed by adding 10 ml of DMEM and centrifuging at 3750 rpm for 10 min at 4°C (with mild braking). The pellet was then diluted in a solution of DMEM containing 100 mg/ml OVA (Sigma-Aldrich) at a concentration of 10^5 RBC/μl and incubated at 37°C for 30 min. Cells were washed three times in PBS before being added to the DC cultures.

To coat RBC with PbA Ag, the concentration of parasites in a blood sample of an infected B6 donor mouse was estimated before lysing by three consecutive cycles of freezing/thawing in liquid nitrogen followed by passage through a 30-gauge needle six times. The equivalent of one parasite per RBC was added to the RBC/OVA solution.

Generation of bone marrow chimeras

B6 mice were irradiated with two doses of 550 rad 3 h apart and reconstituted 4 h later with 5×10^6 bone marrow cells. These were collected from B6 and CD11c-DTR donor mice and depleted of T cells by coating with Abs against CD4 (RL172), CD8 (3.168), and Thy1 (J1j) followed by incubation with rabbit complement for 20 min at 37°C. One day later, mice were injected i.p. with anti-Thy1 Ab (T24) to deplete residual T cells. Chimeric mice were rested for 8–10 wk before use, receiving water containing 2.5 g/l neomycin sulfate and 0.94 g/l polymyxin B sulfate for the first 6 wk after irradiation.

T cell isolation and in vivo proliferation assay

$CD4^+$ or $CD8^+$ T cells were negatively enriched from the spleens and lymph nodes (LNs) of PbT-I/uGFP, PbT-II/uGFP, gDT-II/Ly5.1 or OT-II/Ly5.1 transgenic mice as previously described (57) and labeled with CellTrace Violet (CTV) or CFSE following the manufacturer's instructions (Thermo Fisher). Purified cells (1×10^6) were injected i.v. in 0.2 ml of PBS a day before mice were infected with malaria parasites (10^4, 10^5, or 10^6 iRBC or 5×10^4 RAS, as stated in the figure legend) or HSV (10^5 PFU

HSV). Spleens were harvested at various time points postinfection for the analysis of transgenic TCR cell proliferation by flow cytometry.

To deplete endogenous $CD4^+$ T cells before adoptive transfer, mice were injected i.v. with 100 μg of anti-CD4 Ab (clone GK1.5) 7 and 4 d prior to the transfer of PbT-II cells.

In vitro proliferation assay

Spleens were isolated from naive B6 or BALB/c mice, or B6 mice that had been infected with 10^6 PbA iRBC 3 d earlier, and DC were enriched by a 1.077 g/cm^3 Nycodenz density centrifugation. DC ($1.5–2 \times 10^5$) and $0.6–1 \times 10^5$ CTV-labeled PbT-II cells were incubated with titrated amounts of *P. falciparum* schizonts or PbA iRBC, or with 8×10^6 *T. gondii* tachyzoites, PbA iRBC, uninfected mouse or human RBC, or 2.5×10^5 control HFF cells (the approximate number of host cells required to make 8×10^6 *T. gondii* tachyzoites), for 3 d. Ags were lysed by three consecutive cycles of freezing/thawing in liquid nitrogen followed by passage through a 29-gauge needle six times to facilitate uptake by DC. PbT-II proliferation was assessed by flow cytometry.

Flow cytometry

Cells were labeled with mAbs specific for CD8 (clone 53-6.7), CD4 (RM 4-5), Thy1.2 (30-H12), MHC II (M5/114.15.2), CD11c (N418), CD45.1 (A20), Vα2 (B20.1), Vβ12 (MR11-1), Vα8.3 (B21.14), Vβ10 (B21.5) or CD69 (H1.2F3), Sirpα (P84), T-bet (4B10), Bcl6 (K112-91), Foxp3 (FJK-165), GATA3 (L50-823), retinoic acid–related orphan receptor (ROR)γt (Q31-378). Dead cells were excluded by propidium iodide staining. Cells were analyzed by flow cytometry on a FACSCanto or LSRFortessa (BD Biosciences), using the FlowJo software (Tree Star).

For intracellular staining, cells were permeabilized using a transcription factor buffer set (BD Biosciences) following the manufacturer's instructions. Dead cells were excluded using Live/Dead fixable dead cell stain (Thermo Fisher).

For the determination of parasitemia, 1–2 μl of blood was collected from the tail vein, diluted in FACS buffer (containing 1% w/v BSA and 5 mM EDTA) and incubated at 37°C, 6.5% CO_2 with 5 μg/ml Hoechst 33258 (Thermo Fisher) for 1 h before running on an LSRFortessa. Blood from naive mice was used as negative control (background stain usually ranged between 0.10 and 0.14%)

Generation and monitoring of ECM

Mice infected with blood-stage PbA were monitored daily for the development of ECM. Mice were considered to have ECM when showing signs of neurologic symptoms such as ataxia and paralysis, evaluated as the inability of mice to self-right.

Detection of P. chabaudi*–specific Ab*

Nunc-Immuno MicroWell 96-well ELISA plates (300 μl round-bottom) were coated overnight at 4°C with 50 μl of PBS containing *P. chabaudi* blood-stage lysate (equivalent to 6.6×10^5 parasites per well). Unbound Ag was washed away by soaking the plates in 0.05% Tween 20/PBS (i.e., wash) four times. The wells were blocked with 50 μl of 5% skim milk/PBS for 15–30 min. Plasma samples were serially diluted in 5% skim milk/PBS and incubated overnight at 4°C. The wells were washed six times with 0.05% Tween 20/PBS and incubated overnight at 4°C with 50 μl of 5% skim milk/PBS containing anti-mouse IgG-HRP (1:10,000) to assess the total IgG responses. The wells were washed six times with 0.05% Tween 20/PBS and HRP was detected by adding 50 μl of ABTS substrate in the wells and incubating for 1.5–2 h at room temperature. OD at 405 nm and the background at 492 nm were determined using an ELISA plate reader. The end-point titers were calculated by using cutoff values determined as 2 × SD above average OD at 405–492 nm values of control wells containing no plasma.

P. chabaudi Ag used to coat ELISA plates was prepared as follows: Blood from *P. chabaudi*–infected mice was incubated with 0.05% saponin for 3 min at room temperature to release parasites from RBC. Parasites were then broken up by snap freezing in liquid nitrogen and thawing three times, followed by six passages through a 30-gauge needle.

Statistical analysis

Data were log transformed for conversion into a normal distribution and then analyzed using parametric statistical tests such as a *t* test for the comparison of two groups or ANOVA followed by a Tukey multiple comparison test for simultaneous comparison of multiple groups. A p value < 0.05 was considered statistically significant ($*p < 0.05$, $**p < 0.01$, $***p < 0.001$).

Results

Generation of an MHC II–restricted T cell hybridoma specific for PbA

To study the $CD4^+$ T cell response to blood-stage malaria, we developed an MHC II–restricted T cell hybridoma specific for PbA. This hybridoma, termed D78, was derived by fusing the immortalized cell line BWZ36.GFP (58) to $CD4^+$ T cells isolated from the spleen of a B6 mouse infected with blood-stage PbA. To assess MHC restriction of D78, DC deficient in MHC I or MHC II molecules were preincubated with lysate of PbA iRBC and then tested for stimulatory capacity (Fig. 1A). Whereas both WT and MHC I knockout (KO) DC were able to efficiently stimulate this hybridoma, $I\text{-}A^b$–deficient (MHC II KO) DC were nonstimulatory. In contrast, MHC II KO DC were able to stimulate a PbA-specific MHC I–restricted hybridoma (16), showing that these DCs were functional (Supplemental Fig. 1A). Furthermore, D78 responded efficiently to PbA iRBC lysate, but failed to respond to DCs activated by nonspecific stimuli such as LPS, polyinosinic-polycytidylic acid [poly(I:C)], or CpG, thus excluding self-reactivity or reactivity to FCS proteins (Fig. 1B). Taken together, these findings indicated that the D78 hybridoma was MHC II restricted and specific for malaria Ag.

Generation of a PbA-specific TCR transgenic line

To enable monitoring of $CD4^+$ T cell immunity to PbA in vivo, an MHC II–restricted TCR transgenic mouse line was developed using the TCR α- and β-chains expressed by D78. This line has been termed PbT-II, consistent with our nomenclature for MHC I– and II–restricted OVA-specific lines OT-I and OT-II and our

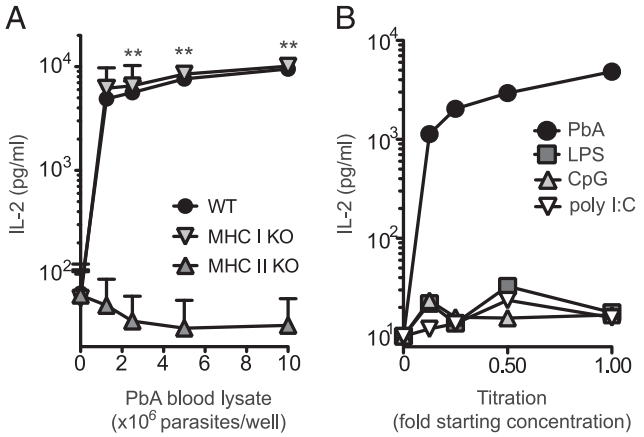

FIGURE 1. Characterization of the D78 hybridoma. (**A**) MHC II restriction. DC were enriched from the spleens of WT B6 (filled circle), MHC I–deficient (inverted triangle), or MHC II–deficient (upright triangle) mice and cultured for 1 h with titrated amounts of lysed blood-stage PbA iRBC before adding 5×10^4 D78 hybridoma cells. Forty hours later, IL-2 concentrations in the supernatants were measured by ELISA. Data points denote mean of IL-2 concentration and error bars represent SEM. Data were pooled from two independent experiments with a total of two to three samples per dose. Statistical analysis was performed on log-transformed data using unpaired *t* tests. $**p < 0.01$, between WT and MHC II–deficient DC. No statistical differences were found between WT and MHC I–deficient DC. (**B**) D78 hybridoma cells do not respond to nonspecific inflammatory stimuli. WT DC were incubated for 1 h with either blood-stage PbA parasite lysate or the TLR agonists LPS, 1668 CpG, or poly(I:C). Hybridoma cells were then added to the culture and incubated for a further 40 h before IL-2 concentrations in the supernatants were measured by ELISA. Starting concentrations of the stimuli were 4 million parasites per well, 100 ng/ml LPS, 10 nmol/ml CpG, and 1 μg/ml poly(I:C). Data are from one of two representative independent experiments with one sample per dose.

recently reported MHC I–restricted PbA-specific line, termed PbT-I (16). Analysis of the spleen and inguinal LN (iLN) of PbT-II mice revealed skewing toward $CD4^+$ T cells as well as efficient expression of the Vα2 and Vβ12 transgenes derived from D78 (Fig. 2, Supplemental Fig. 1C). Total cellularity in the spleen of PbT-II mice was similar to WT mice, with $CD4^+$ T cells largely compensating for reduced numbers of $CD8^+$ T cells in the former (Supplemental Fig. 1D). Some reduction in the total cellularity of the iLN was evident, but the reason for this is unclear. Of note, increased numbers of $CD4^-CD8^-$ (DN) T cells were also found in the spleen and iLN of PbT-II mice. In the thymus, PbT-II mice showed an increased number and proportion of single-positive $CD4^+$ T cells and DN T cells (Supplemental Fig. 1B, 1D). Similar to previously described TCR transgenic mice, total cellularity was reduced in the thymus, indicative of efficient positive selection (16, 59).

PbT-II cells respond to multiple Plasmodium *species and life-cycle stages*

PbT-II mice were generated without knowledge of their specific peptide Ags. To further characterize the specificity of this line, we tested responsiveness to different species of malaria parasites. CTV-labeled PbT-II cells were adoptively transferred into B6 mice 1 d before infection with iRBC from either PbA, *P. berghei* NK65, *P. chabaudi*, or *P. yoelii* 17XNL. Several days later, PbT-II proliferation was assessed in the spleen, revealing reactivity to all *Plasmodium* species (Fig. 3A). To ascertain whether the observed proliferation ensued from Ag recognition through the transgenic TCR, and not by endogenously rearranged receptors (60), we crossed PbT-II mice to RAG1-deficient mice, which are unable to perform the gene rearrangements required for the generation of endogenous T (and B) cell receptors (43). $CD4^+$ T cells in the spleens of RAG1-deficient PbT-II mice expressed the Vα2 and Vβ12 transgenes (Supplemental Fig. 2A) and, similar to RAG1-sufficient PbT-II $CD4^+$ T cells, were able to respond to PbA, *P. chabaudi* AS, and *P. yoelii* 17XNL (Supplemental Fig. 2B, 2C). These data demonstrated that the transgenic TCR was responsible for parasite recognition.

The broad recognition of murine malaria parasites prompted us to determine whether PbT-II cells also responded to the human malaria parasite *P. falciparum*. In vitro culture of PbT-II cells with DC and *P. falciparum* schizont lysate resulted in PbT-II proliferation comparable to that seen in response to PbA (Fig. 3B), indicating that the Ag recognized by PbT-II cells was conserved in multiple *Plasmodium* species. PbT-II $CD4^+$ T cells did not respond to uninfected mouse or human RBC, human foreskin fibroblast, or *T. gondii* tachyzoites (Supplemental Fig. 2D), suggesting that specificity of this line was limited to *Plasmodium* species.

We then asked whether the Ag recognized by PbT-II cells was also expressed by pre-erythrocytic–stage PbA parasites. To examine this issue, CTV-labeled PbT-II cells were adoptively transferred into B6 mice that were then infected with RAS that do not develop into blood-stage infection. This revealed significant, although weak, proliferation of PbT-II cells 6 d later, indicating some reactivity to the pre-erythrocytic stage of PbA (Fig. 3C).

To confirm that the responsiveness of PbT-II cells observed in vivo was due to the recognition of a malaria parasite–derived epitope, and not to nonspecific inflammatory signals generated by in vivo infection, we transferred gDT-II cells, which are $CD4^+$ T cells specific for HSV, and PbT-II cells into B6 mice that were i.v. infected with 10^5 HSV PFU 1 d later. Whereas gDT-II cells proliferated extensively by day 10 postinfection, PbT-II cells remained undivided (Supplemental Fig. 2E). To further characterize the MHC II restriction of PbT-II cells, these cells were coated with CTV and cultured in vitro with DC from the spleens of B6 ($I\text{-}A^b$) or BALB/c ($I\text{-}A^d$) mice in the presence of titrated amounts of PbA Ag. Unlike DC extracted from B6 mice, $I\text{-}A^d$ BALB/c DC were unable to stimulate PbT-II cells, indicating an exclusive restriction of PbT-II cells for $I\text{-}A^b$ molecules (Supplemental Fig. 2F).

Taken together, these results revealed a broad responsiveness of PbT-II cells to malaria parasites, including different life-cycle stages and species, showcasing the potential for these T cells as tools to broadly study $CD4^+$ T cell responses in malaria.

PbT-II cells can provide immunity to P. chabaudi *infection*

Both B cells and Th cells are essential for the control of *P. chabaudi* parasitemia (61, 62), and protection is mainly achieved by parasite-specific T cell–dependent Abs (17). This model was therefore ideally suited to test whether PbT-II cells have the capacity to provide protective immunity to malaria. We transferred

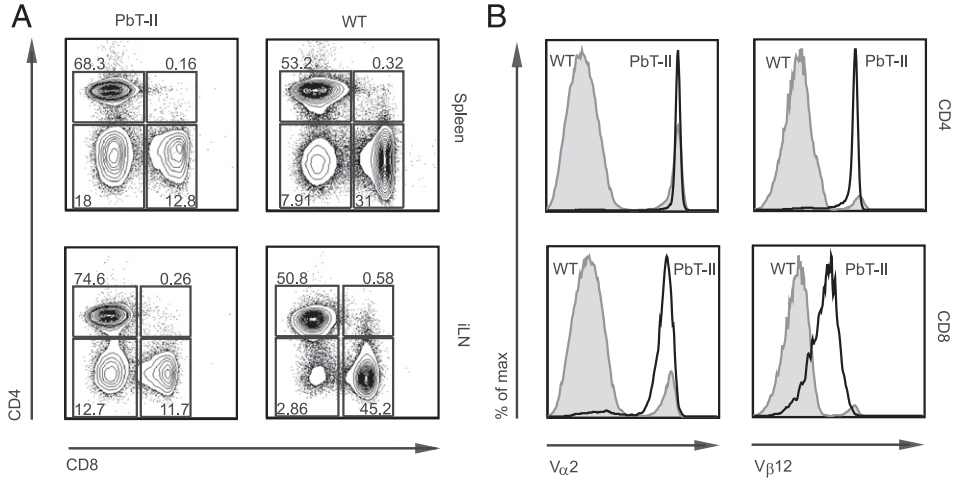

FIGURE 2. Characterization of T cells from the spleen and LN of PbT-II mice. Cells were harvested from the spleen and the LN of PbT-II transgenic or control B6 (WT) mice. FACS analysis was performed to characterize the expression of CD4, CD8, and the transgenic TCR α-chain (Vα2) and β-chain (Vβ12). (**A**) Representative plots showing the proportions of $CD4^+$ versus $CD8^+$ $Thy1.2^+$ cells in the spleen and iLN of PbT-II and WT mice. (**B**) Representative histograms showing the expression of the transgenic TCR Vα2 and Vβ12 chains on the CD4 or CD8 single-positive cells from the spleen. Data are representative of two independent experiments in which at total of six PbT-II and seven WT mice were analyzed.

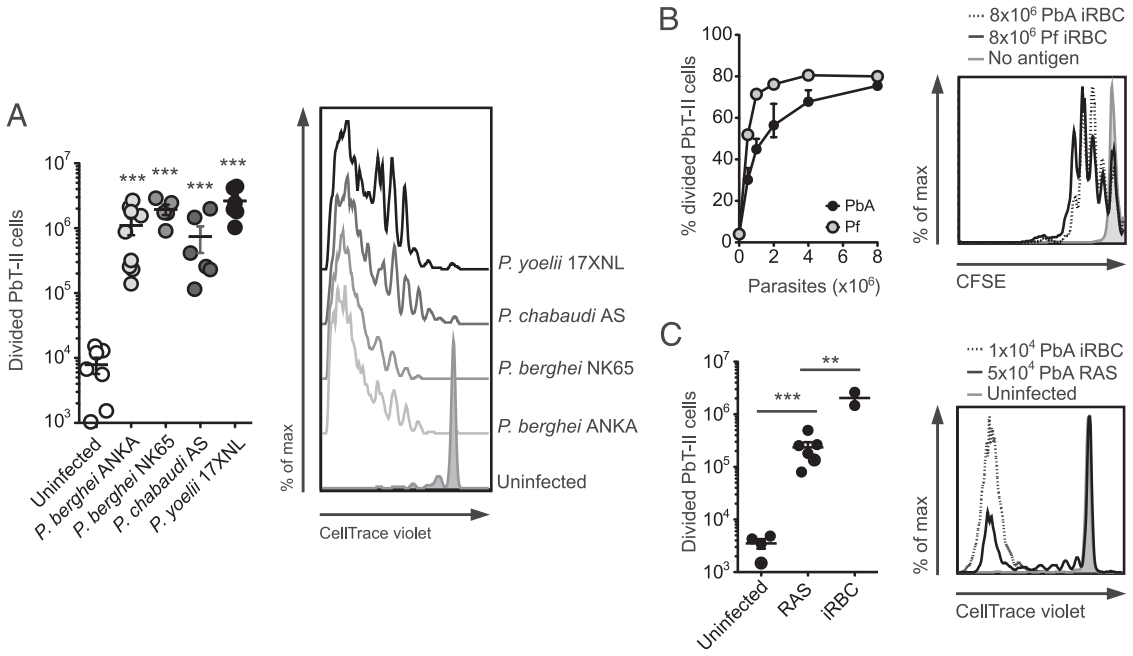

FIGURE 3. PbT-II cells are cross-reactive with multiple *Plasmodium* species and with liver-stage PbA. (**A**) Cross-reactivity with murine malaria parasites. CTV-labeled PbT-II cells (10^6) were transferred into B6 recipients 1 d before infection with 10^4 iRBC from PbA, *P. berghei* NK65, *P. chabaudi* AS, *P. yoelii* 17XNL, or nothing. Five days after PbA and *P. berghei* NK65 infection, or 7 d after *P. chabaudi* AS and *P. yoelii* 17XNL infection, mice were killed and PbT-II proliferation was assessed in the spleen. Left panel, Number of divided cells per mouse. Each point represents an individual mouse. Right panel, Representative histograms showing PbT-II proliferation. Data are pooled from two independent experiments. Data were log transformed and analyzed using one-way ANOVA and a Dunnett multiple comparison test. ***$p < 0.001$, for differences with the uninfected group. (**B**) Cross-reactivity with *P. falciparum*. Splenic DC (2×10^5) were cultured with 10^5 CFSE-coated PbT-II cells and titrated amounts of *P. falciparum* (Pf) or PbA iRBC for 3 d. PbT-II proliferation was assessed by flow cytometry. Left panel, Percentages of proliferating PbT-II cells to Pf or PbA Ag. Right panel, Representative histogram showing PbT-II proliferation to Pf-iRBC (solid black line), PbA iRBC (dotted line), and a negative control containing no Ag (tinted gray line). Data are from one representative experiment of two independent experiments with two samples per dose. (**C**) Cross-reactivity with liver-stage PbA parasites. CTV-labeled PbT-II cells (10^6) were transferred into recipient B6 mice 1 d before infection with 5×10^4 PbA RAS or 10^4 PbA iRBC. Six days later mice were killed and PbT-II proliferation was assessed in the spleen. Left panel, Number of divided cells per mouse. Each point represents an individual mouse. Right panel, Representative histograms showing PbT-II proliferation. The filled histogram represents an uninfected control. The solid and dotted black lines show PbT-II cell proliferation in mice infected with PbA RAS or iRBC, respectively. Data were pooled from two independent experiments. Data were log transformed and analyzed using one-way ANOVA and a Tukey multiple comparison test. **$p < 0.01$, ***$p < 0.001$.

PbT-II cells into CD40L-deficient mice, in which endogenous $CD4^+$ T cells are unable to provide help to B cells (48), and infected these mice with 10^4 *P. chabaudi* iRBC. CD40L-deficient mice lacking PbT-II cells succumbed to infection during the peak of parasitemia on day 9 postinfection, or shortly thereafter, whereas those adoptively transferred with PbT-II cells survived >30 d (Fig. 4A, Supplemental Fig. 3A). These latter mice developed a second peak of parasitemia on day 19 postinfection that occurred earlier and was higher than that of WT mice (Fig. 4B, Supplemental Fig. 3A). Although parasitemia was still detectable on day 26 postinfection, CD40L-deficient mice that received PbT-II cells had recovered from disease symptoms, as revealed by increased body weight to preinfection levels (Supplemental Fig. 3A), and were sacrificed >50 d postinfection without signs of disease. Analysis of the plasma of these mice on day 9 postinfection also revealed increased levels of *P. chabaudi*–specific IgG in CD40L-deficient mice that received PbT-II cells compared with those that did not receive cells (Fig. 4C).

The protective effect of PbT-II cells for *P. chabaudi* infection was not limited to the production of Abs, as adoptive transfer of PbT-II cells into RAG1-deficient mice, which are devoid of T cells and B cells, also resulted in a significantly prolonged survival (Fig. 4A). The first peak of parasitemia, on day 9 postinfection, was significantly higher in RAG1-deficient mice that did not receive PbT-II cells than in WT mice and RAG1-deficient mice that received PbT-II cells (Fig. 4B, Supplemental Fig. 3A). Unlike as seen for CD40L-deficient mice, however, PbT-II cells did not enable RAG1-deficient mice to fully control parasitemia and these mice eventually succumbed to infection (Fig. 4A, 4B, Supplemental Fig. 3A).

These results clearly show that PbT-II cells promoted immunity against *P. chabaudi* infection via Ab production and Ab-independent mechanisms that contributed to the control of parasitemia.

$CD8^+$ DC are the main APC for PbT-II cells

Previous reports using DC from infected mice ex vivo have implicated both $CD8^+$ and $CD8^-$ DC in MHC II–restricted Ag presentation during blood-stage malaria infection (9, 39, 63). To examine the capacity of cDC subsets to present malaria Ags to $CD4^+$ T cells, we enriched cDC (defined as $CD11c^{hi}$MHC II^{hi} cells) from the spleens of naive mice and subdivided them into three subsets: $CD8^+CD4^-$, $CD8^-CD4^+$, and $CD8^-CD4^-$ DC ($CD8^+$, $CD4^+$, and DN DC, respectively) (64). $CD8^+$ DC also express XCR1 (46), Clec9A (65), CD24, and DEC205 (64), and lack expression of Sirpα (Supplemental Fig. 3B). $CD4^+$ DC are the most abundant of the three subtypes (making up ~55% of all cDC) and express CD11b (64) and Sirpα (Supplemental Fig. 3B). DN DC are a heterogeneous group of DC in which most cells express Sirpα and CD11b, but a small group lack Sirpα (Supplemental Fig. 3B), likely cDC precursors (66). We incubated purified DC subtypes with PbA iRBC and the D78 hybridoma

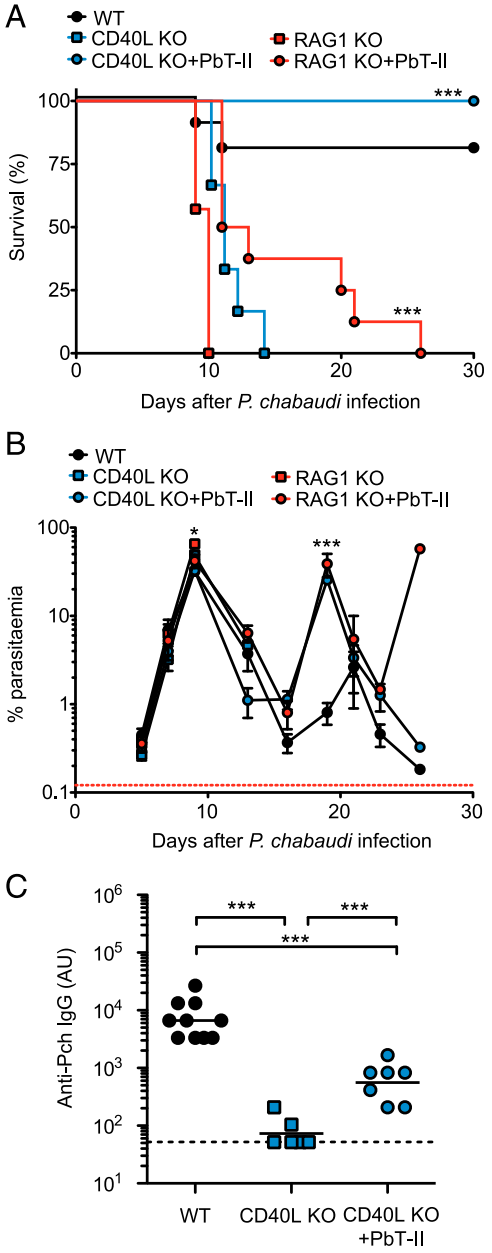

FIGURE 4. PbT-II cells can elicit immunity to *P. chabaudi* infection. CD40L-deficient mice (CD40L KO), RAG1-deficient mice (RAG1 KO), and WT control mice received either 5×10^5 PbT-II cells or no cells 1 d before infection with 10^4 *P. chabaudi* iRBC. (**A**) Survival of WT mice (n = 10), CD40L-deficient mice with or without PbT-II cells (n = 7 and 6, respectively), and RAG1 KO mice with or without PbT-II cells (n = 8 and 7, respectively). Data were analyzed using log-rank test. ***$p < 0.001$, between CD40L KO versus CD40L KO plus PbT-II mice and RAG1 KO versus RAG1 KO plus PbT-II mice, respectively. (**B**) Course of parasitemia after *P. chabaudi* infection. Blood samples from mice in (A) were examined by FACS and mean parasitemia was graphed. The dotted red line represents background staining in uninfected mice. Data were log transformed and analyzed using one-way ANOVA and a Tukey multiple comparison test. A statistical difference was found on day 9 between RAG1 KO and RAG1 KO plus PbT-II mice (*$p < 0.05$). No difference was found between CD40L KO and CD40L KO plus PbT-II mice on day 9. Statistically significant differences between both CD40L KO plus PbT-II or RAG1 KO plus PbT-II mice and WT mice were found on day 19 (***$p <$ 0.001). (**C**) Parasite-specific IgG Abs in CD40L KO mice. *P. chabaudi*–specific IgG end-point titers were determined on day 9 postinfection using ELISA. Cut-off values were determined as 2 × SD above average OD at 405–492 nm values of control wells containing no plasma. Data were log transformed and analyzed using a one-way ANOVA and a Tukey multiple comparison test (***$p < 0.001$). The dotted line represents the limit of detection of the assay.

in vitro and assessed the hybridoma responses (Fig. 5A). Although all three DC subsets were capable of stimulating D78, their efficacy varied considerably: $CD8^+$ DC induced the strongest responses; DN DC had an intermediate stimulatory capacity; and $CD4^+$ DC were significantly less efficient than any of the other subtypes. A similar result was obtained when the three cDC subsets were purified from the spleens of B6 mice that had been infected with PbA 3 d earlier (Fig. 5B). In this case, the stimulation exerted by DN DC and $CD4^+$ DC was comparable and significantly lower than that of $CD8^+$ DC.

It was possible that the observed superiority of $CD8^+$ DC was due to the characteristics of the specific peptide recognized by the D78 hybridoma, and not generalizable to other peptides. To clarify this point, we sought to test the capacity of cDC subsets at presenting OVA to the OT-II hybridoma in vitro. Consistent with previous studies (34), incubation of $CD4^+$, $CD8^+$, and DN DC with soluble OVA demonstrated a comparable capacity of all these DC to stimulate the OT-II hybridoma (Fig. 5C). However, because the form of the Ag influences the effectiveness of its capture and processing by DC (34), and the malaria parasite Ag used to assess D78 responses in vitro in Fig. 5A was cell associated (i.e., from iRBC), we coated RBC from a naive B6 mouse with OVA in an attempt to provide this Ag to DC in a comparable, cell-associated fashion. Similar to the dominance of $CD8^+$ DC in presentation of iRBC malaria Ag to D78, these DC were the most efficient stimulators of the OT-II hybridoma when OVA-coated RBC were used (Fig. 5D). $CD4^+$ DC were the least efficient DC subtype, and DN DC exhibited an intermediate stimulatory capacity.

Taken together, these results indicate that $CD8^+$ DC have the highest capacity for stimulation of the D78 hybridoma and suggest that this DC subset is particularly efficient at presenting MHC II–restricted Ags associated with RBC.

To validate the role of $CD8^+$ DC in vivo, we then took advantage of the PbT-II TCR transgenic mice, which enabled us to follow the response of adoptively transferred PbT-II T cells in mice lacking DC. Although DC are efficient APC capable of activating $CD4^+$ T cells, other cells can present Ag via MHC II and can therefore contribute to $CD4^+$ T cell priming (67). To assess the contribution of DC in the priming of PbT-II cells during PbA infection, we first reconstituted lethally irradiated B6 mice with bone marrow from CD11c-DTR mice. In these chimeras, DC could be depleted by the administration of DT (47). Consistent with previous reports (9, 68), DT treatment of CD11cDTR→B6 chimeras during PbA infection resulted in the complete abrogation of PbT-II cell proliferation (Fig. 6A, 6E), demonstrating an essential role of DC in $CD4^+$ T cell priming during blood-stage infection. A similar result was obtained when DC were removed after *P. chabaudi* infection (Supplemental Fig. 3C).

To assess the role of individual DC subsets in the PbT-II response, we examined reactivity in mice deficient in subsets of DC due to the lack of specific transcription factors, namely Batf3 (44) or IRF8 (45). Batf3-deficient mice contain all DC subsets except $CD8^+$ DC and their migratory equivalents, the $CD103^+$ DC, and have been shown to sustain low $CD8^+$ T cell proliferation after PbA infection (69). However, on a B6 background, some $CD8^+$ DC can be found in the LN of Batf3-deficient mice (70) and precursors capable of MHC II–restricted presentation but not cross-presentation are found in the spleen (71). To examine the PbT-II response in Batf3-deficient mice, CTV-labeled PbT-II cells were adoptively transferred 1 d before infection with 10^4 PbA

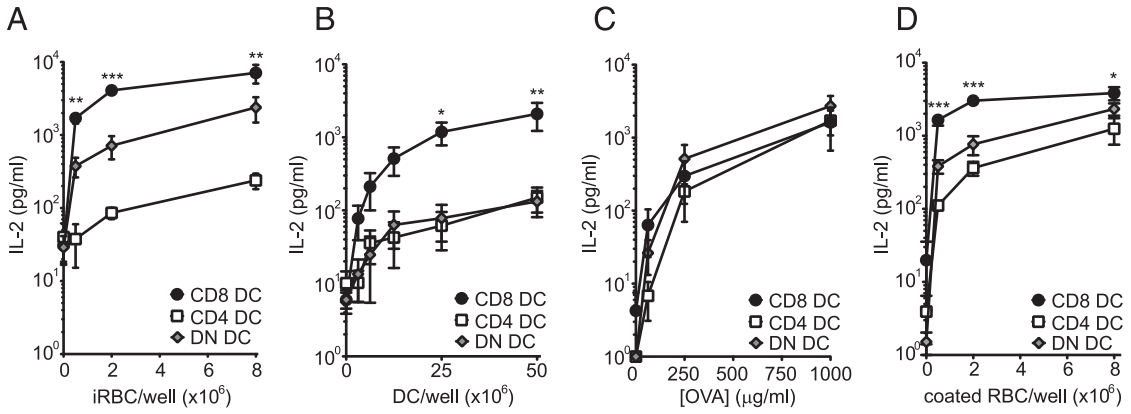

FIGURE 5. $CD8^+$ DC are more efficient than other DC subtypes at stimulating D78 hybridoma cells in vitro and ex vivo. (**A**) D78 stimulation by DC subtypes in vitro. Sorted $CD4^+$, $CD8^+$, or DN DC (5×10^4) from naive B6 mice were preincubated for 1 h with titrated amounts of PbA iRBC. D78 hybridoma cells (5×10^4) were then added to the culture and incubated for a further 40 h before supernatants were collected and IL-2 concentrations measured by ELISA. (**B**) D78 stimulation by DC subtypes ex vivo. Sorted $CD4^+$, $CD8^+$, or DN DC (5×10^4) from the spleens of B6 mice infected with 10^6 PbA iRBC 3 d earlier were incubated with 5×10^4 D78 hybridoma cells for 40 h before supernatants were collected and IL-2 concentrations measured by ELISA. (**C**) Presentation of soluble OVA Ag to the OT-II hybridoma. Sorted $CD4^+$, $CD8^+$, or DN DC (5×10^4) from naive B6 mice were preincubated for 1 h with titrated amounts of soluble OVA. OT-II hybridoma cells (5×10^4) were then added to the culture and incubated for a further 40 h before supernatants were collected and IL-2 concentrations measured by ELISA. (**D**) $CD8^+$ DC are more efficient than other DC subtypes at presenting RBC-associated Ag to the OT-II hybridoma in vitro. Sorted $CD4^+$, $CD8^+$, or DN DC (5×10^4) from naive B6 mice were preincubated for 1 h with OVA-coated RBC from a naive B6 mouse. OT-II hybridoma cells (5×10^4) were then added to the culture and incubated for a further 40 h before supernatants were collected for assessment of IL-2 concentrations by ELISA. Data were pooled from three independent experiments in (A)–(C) and from four independent experiments in (D), with a total of three to four samples per data point. Data were log-transformed and statistically analyzed using one-way ANOVA. $*p < 0.05$, $**p < 0.01$, $***p < 0.001$.

iRBC. PbT-II proliferation was then assessed 5 d later (Fig. 6B, 6E). This showed that the total number of proliferating PbT-II cells was reduced in Batf3-deficient mice (Fig. 6B), and pairwise comparisons showed a 50% reduction relative to WT controls (Fig. 6E). These findings indicated that PbT-II cells were heavily dependent on mature $CD8^+$ DC for Ag presentation, but suggested some participation by other DC, possibly the less mature form of $CD8^+$ DC present in Batf3-deficient spleens (incapable of cross-presentation) or an alternative $CD8^-$ DC subset.

IRF8-deficient mice are profoundly deficient in $CD8^+$ DC, $CD103^+$ DC, and plasmacytoid DC, but contain other cDC subsets, so these mice represent an ideal host for assessing the role of $CD8^-$ cDC in Ag presentation. CTV-labeled PbT-II cells were therefore adoptively transferred into IRF8-deficient mice 1 d before infection with PbA iRBC and T cell proliferation assessed 5 d later (Fig. 6C, 6E). PbT-II proliferation was severely reduced in these mice (Fig. 6C), amounting to ~20% of WT responses (Fig. 6E), further supporting the major role for $CD8^+$ DC in PbT-II responses.

Lack of IRF8 is known to result in immune defects in addition to the absence of $CD8^+$ DC, for example, $CD8^-$ DC, although in normal numbers, are hyporesponsive to microbial stimulation (72). Also, IRF8-deficient mice show an excessive production of granulocytes resulting in splenomegaly (45), which could have hindered proper priming and proliferation of PbT-II cells. Thus, to further explore the importance of $CD8^+$ DC in PbT-II priming to PbA, we assessed PbT-II proliferation in DT-treated XCR1-DTRvenus mice. XCR1 is a chemokine receptor expressed by mature $CD8^+$ DC and by their migratory $CD103^+$ counterparts, found in LN. DT treatment of XCR1-DTRvenus mice, which express the DT receptor under the XCR1 promoter, results in the elimination of $CD8^+$ DC from the spleen (46). Consistent with the results obtained using IRF8-deficient mice infected with blood-stage PbA, PbT-II proliferation was significantly reduced in the spleen of DT-treated XCR1-DTRvenus mice, amounting to ~30% of WT controls (Fig. 6D, 6E).

Taken together, these data demonstrated an essential role for DC in the generation of PbT-II cell responses to blood-stage malaria parasites and argued that the $CD8^+$ DC subtype played a dominant role.

$CD8^+$ DC influence Th1 and follicular Th cell induction

DC subsets can influence the expression of transcription factors by T cells and drive their differentiation into particular Th phenotypes (35, 36, 73–75). To address the role of $CD8^+$ DC on the differentiation of PbT-II cells after PbA infection, XCR1-DTRvenus mice were adoptively transferred with PbT-II cells and then infected with 10^4 PbA iRBC. These mice were either treated with DT throughout the infection to remove $CD8^+$ DC or given PBS, maintaining this DC subset. On day 7, the expression of transcription factors that define Th1, Th2, Th17, follicular Th (Tfh), and regulatory T cell subsets (i.e., T-bet, GATA3, RORγt, Bcl6, and Foxp3, respectively) was assessed in PbT-II cells, revealing induction of $T\text{-bet}^+$ and $Bcl6^+$ PbT-II cells, which was impaired upon depletion of $CD8^+$ DC (Fig. 6F, Supplemental Fig. 3D). No expression of GATA3, RORγt, or Foxp3 was detected in PbT-II cells, even in the presence of $CD8^+$ DC. A similar dependence on $CD8^+$ DC for Th1 and Tfh cell development was observed for endogenous $CD4^+$ T cells (Fig. 6F). Of note, and agreeing with a previous study (75), the proportion of $T\text{-bet}^+$ $CD8^+$ T cells was also markedly reduced in mice depleted of $CD8^+$ DC. These results suggested a major role for $CD8^+$ DC in promoting T-bet expression in CD4 and CD8 T cells, and a lower, but significant, contribution to the generation of Tfh cells.

$CD8^+$ DC function early after infection is essential for ECM development

In vitro experiments involving the use of transgenic parasites expressing model Ags previously showed that $CD8^+$ T cell priming during blood-stage malaria parasite infection is efficiently performed by $CD8^+$ DC, but only poorly by other DC subsets (9). To confirm this point in vivo, we transferred $CD8^+$ T cells from the

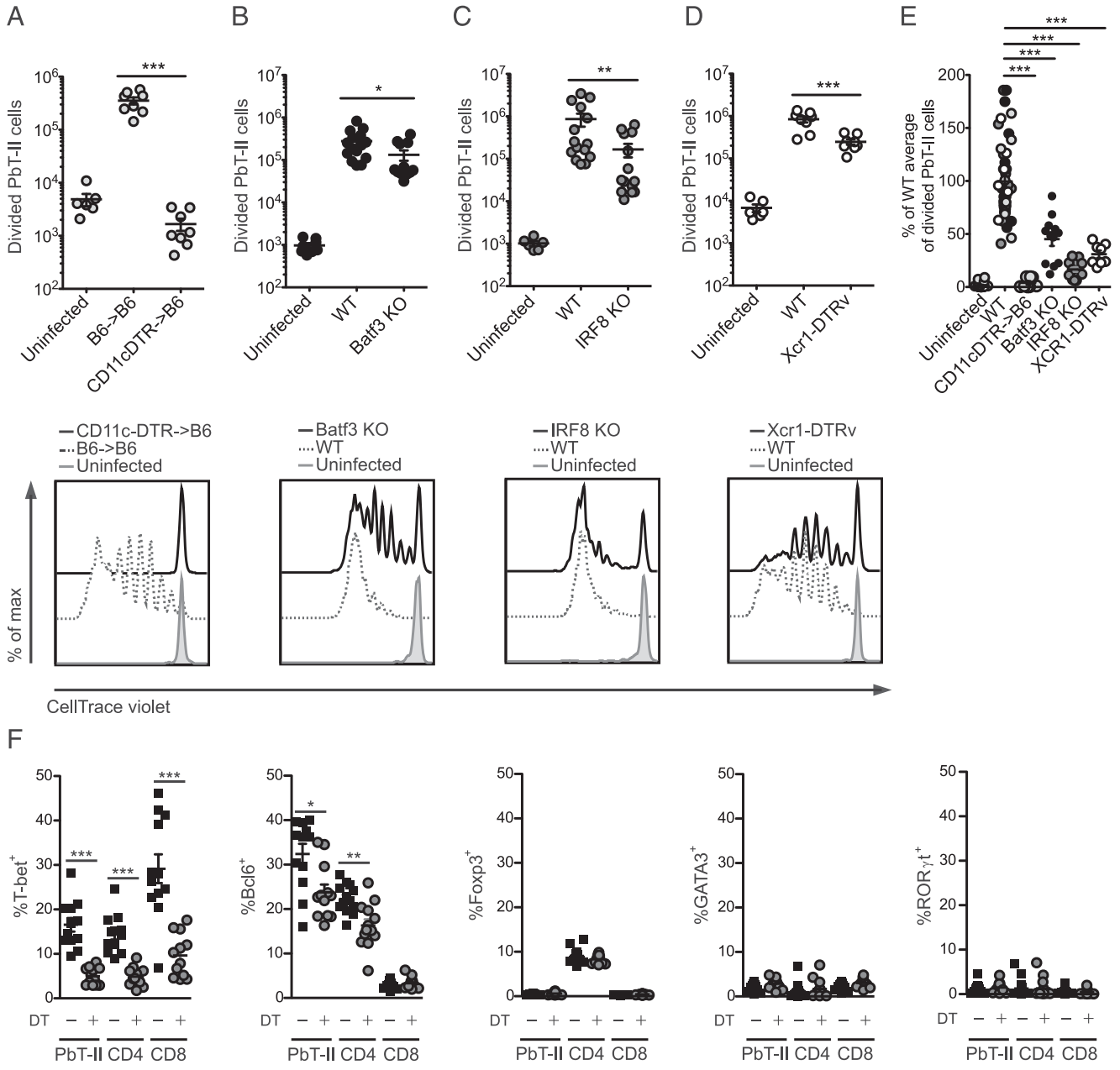

FIGURE 6. PbT-II priming during blood-stage PbA infection is exclusively done by DC, among which the $CD8^+$ subset is the major contributor. CTV-labeled PbT-II cells (10^6) were adoptively transferred into different DC deficient recipient mice or WT controls, which were infected with 10^4 PbA iRBC 1–2 d later. Proliferation of PbT-II cells was measured in the spleen on day 5 after PbA infection. Total divided cells in the spleen (upper graph, each point represents an individual mouse) and the corresponding representative histograms for proliferation (below) are shown in each subfigure. The different groups in the upper graph are represented in the histograms below as solid black lines (DC deficient mice), dotted lines (WT control mice), and filled gray lines (uninfected mice). (**A**) PbT-II proliferation in DT-treated B6→B6 or CD11c-DTR→B6 chimeras. Mice were treated with 100 ng of DT i.p. on days −1, 1, and 3 postinfection. (**B**) PbT-II proliferation in WT or Batf3 KO mice. (**C**) PbT-II proliferation in WT or IRF8 KO mice. (**D**) PbT-II proliferation in DT-treated WT or XCR1-DTRvenus mice. Mice were treated with 500 ng of DT i.p. on days −1, 0, 1, and 2 postinfection. Data were pooled from two independent experiments in (A) and (D), and three independent experiments in (B) and (C). For statistical analysis, data were log transformed and analyzed using one-way ANOVA followed by a Tukey multiple comparison test. $*p < 0.05$, $**p < 0.01$, $***p < 0.001$. (**E**) Percentages of PbT-II proliferation in DC-deficient mice compared with their WT counterparts. Data derived from (A) to (D) were normalized to facilitate comparisons between individual experiments. First, the average of divided PbT-II cells in WT mice in each experiment was calculated. That number was then used to calculate the percentage of PbT-II divided cells in both KO mice (CD11cDTR→B6, light gray circles; Batf3 KO, black circles; IRF8 KO, dark gray circles; XCR1-DTRvenus mice, white circles) or their respective WT counterparts (whose normalized proliferation would therefore average 100%). Each point represents an individual mouse. Data in (E) were statistically compared using a Kruskal–Wallis tests followed by a Dunn multiple comparisons test for differences between the individual groups. $***p < 0.001$. (**F**) Transcription factor expression in splenic PbT-II cells and endogenous $CD4^+$ and $CD8^+$ T cells primed in the presence or absence of $CD8^+$ DC. XCR1-DTRvenus mice received 5×10^5 PbT-II/uGFP cells and were infected with 10^4 PbA iRBC 1 d later. These mice were treated with either DT (500 ng/dose) or PBS on days −1, 0, 1, 2, 4, and 6 postinfection and killed on day 7. Data points represent individual mice that were pooled from two independent experiments, log transformed, and statistically analyzed using an unpaired *t* test. $*p < 0.05$, $**p < 0.01$, $***p < 0.001$. Data are represented as mean ± SEM.

PbT-I transgenic line into Batf3-deficient mice or XCR1-DTRvenus mice and then infected these mice with PbA. XCR1-DTRvenus mice were treated with DT from days −1 to 2 postinfection to specifically remove $CD8^+$ DC. PbT-I proliferation was severely decreased in the absence of $CD8^+$ DC in both cases (Supplemental Fig. 4A, 4B), confirming the important role of this DC subtype in $CD8^+$ T cell activation during blood-stage PbA infection.

To assess the role of $CD8^+$ DC in ECM, we first assessed ECM in Batf3-deficient mice after infection with 10^4 PbA iRBC (Supplemental Fig. 4C). In agreement with previous reports (69), Batf3-deficient mice did not develop ECM, demonstrating an essential role for $CD8^+$ DC in promoting pathology. To obtain a precise indication of the temporal requirement for $CD8^+$ DC, we treated XCR1-DTRvenus mice with DT during the early stages of PbA infection (days −1 to 2 postinfection) and monitored for ECM. Whereas nondepleted mice rapidly succumbed to ECM, DT-treated mice were largely protected (Supplemental Fig. 4D), despite harboring similar levels of parasitemia (Supplemental Fig. 4F). To determine whether $CD8^+$ DC function may be required during the effector phase of ECM, XCR1-DTRvenus mice were infected with PbA and treated with DT from day 5 postinfection (Supplemental Fig. 4E). In contrast to mice depleted of DC from the beginning of infection, all mice depleted just prior to ECM onset showed rapid disease onset, supporting the view that $CD8^+$ DC were essential for the priming but not the effector phase of ECM.

$CD4^+$ T cell help acting on $CD8^+$ DC is required for $CD8^+$ T cell priming during blood-stage PbA infection

Primary $CD8^+$ T cell responses can be $CD4^+$ T cell–dependent (18) or –independent (19–21). To study the relevance of $CD4^+$ T cell help during blood-stage malaria, we looked at the expansion of $CD8^+$ PbT-I cells in the absence of $CD4^+$ T cells. We transferred 1 million CTV-labeled PbT-I cells into MHC II–deficient mice, devoid of $CD4^+$ T cells, and infected them with 10^4 PbA iRBC. PbT-I proliferation 5 d later was significantly reduced in MHC II–deficient mice compared with their WT counterparts (Fig. 7A). Because elevated numbers of $CD8^+$ T cell precursors can reduce helper requirements (76), transfer of a high number of PbT-I cells (1 million per mouse) in the previous experiment might have resulted in an artificial enhancement of T cell proliferation in the mice lacking CD4 T cells. To clarify this point, we transferred lower numbers of PbT-I cells (10^5, 10^4) into MHC II–deficient mice, infected them with 10^4 PbA iRBC, and examined proliferation on day 5. This revealed that for this infection model, the response of PbT-I cells was similarly reduced in MHC II–deficient mice compared with WT counterparts regardless of the initial number of PbT-I cells transferred (Fig. 7B).

Because signals derived from parasite material can promote DC licensing (22), we reasoned that infection with higher numbers of parasites might result in a decreased need for $CD4^+$ T cell help. To examine this issue, mice depleted of $CD4^+$ T cells with the mAb GK1.5 (as an alternative to MHC II–deficient mice) were adoptively transferred with 10^6 CTV-labeled PbT-I cells and then infected with 10^4, 10^5, or 10^6 PbA iRBC. Although numbers of divided PbT-I cells were significantly reduced in $CD4^+$ T cell–depleted mice compared with nondepleted controls for all parasite doses, the proportional difference was largest for the lower doses (Fig. 7C). This indicated that the requirement for help during blood-stage infection with PbA was somewhat affected by the infection dose.

Licensing of DC for CTL immunity requires the interaction of costimulatory molecules between activated $CD4^+$ T cells and DC. CD40L (on the $CD4^+$ T cell) and CD40 (on the DC) have been shown to mediate DC licensing in several infectious and noninfectious settings (77–79). To determine whether this pathway was relevant for the provision of help by $CD4^+$ T cells during blood-stage PbA infection, we transferred PbT-I cells into either mice lacking CD40 or CD40L and infected them with 10^4 iRBC. PbT-I proliferation and total numbers were significantly reduced in the spleens of both CD40-deficient and CD40L-deficient mice relative to WT controls (Fig. 7D). Taken together, the results demonstrated a need for $CD4^+$ T cells and CD40–CD40L interactions for the development of optimal $CD8^+$ T cell responses during infection with blood-stage malaria.

To demonstrate that $CD4^+$ T cells provide help via CD40–CD40L interactions to promote optimal $CD8^+$ T cell activation during blood-stage PbA infection, we adoptively transferred 10^6 WT PbT-II cells together with 10^6 PbT-I cells into CD40L-deficient mice (in which endogenous $CD4^+$ T cells were unable to license DC) and then infected these mice with 10^4 iRBC. Whereas PbT-I proliferation was reduced in CD40L-deficient mice, their response was recovered to WT levels in mice that received PbT-II cells (Fig. 7E). To assess the capacity of PbT-II cells to help $CD8^+$ T cells cause ECM, we examined the influence of PbT-II cells on the onset of ECM in CD40L-deficient mice. Although CD40L-deficient mice showed a significant delay in ECM onset compared with WT mice, this delay was alleviated by transfer of PbT-II cells (Fig. 7F). Changes in the time frame for ECM development were independent of parasitemia, which was not significantly altered by the adoptive transfer of PbT-II cells (Supplemental Fig. 4G). Taken together, these results showed that PbT-II cells were able to help $CD8^+$ T cells proliferate and cause ECM in CD40L-deficient mice.

In summary, our results indicate that $CD8^+$ DC are the main APC priming both $CD4^+$ and $CD8^+$ T cells during infection with blood-stage PbA parasites. Using our newly generated PbT-II transgenic mouse line, we demonstrated that optimal expansion of $CD8^+$ T cells required $CD4^+$ T cell help, which was provided to the DC via CD40–CD40L interactions.

Discussion

Although TCR transgenic mouse lines are very useful for deciphering the mechanisms by which T cells operate and carry out their functions in different contexts of infection, the available range of these lines specific for blood-stage malaria Ags is limited. In this study, we describe a $CD4^+$ T cell transgenic mouse line, termed PbT-II, specific for a broad range of *Plasmodium* species and responsive to both blood-stage and pre-erythrocytic stage infections, offering wide applicability for the study of $CD4^+$ T cell function in multiple malaria models. To date, the only available $CD4^+$ TCR transgenic murine line specific for malaria parasites (*P. chabaudi*) was B5, which is restricted to $I\text{-}E^d$ and therefore only usable in the BALB/c background. The PbT-II mice provide the opportunity to analyze *Plasmodium*-specific $CD4^+$ T cells on the B6 background, for which availability of reagents and gene-deficient mice is much broader. We show in the present study that PbT-II cells are an excellent tool for studying $CD4^+$ T cell function in the context of malaria immunity or pathology. When adoptively transferred into CD40L-deficient mice, in which endogenous $CD4^+$ T cells are unable to fully activate B cells or DC (49, 77, 79), PbT-II cells were able to replace endogenous $CD4^+$ T cells for the generation of both Ab responses, which allowed control of *P. chabaudi* parasitemia, and $CD8^+$ T cell responses, which caused ECM after PbA infection. This indicates that PbT-II cells are an invaluable tool for the study of $CD4^+$ T cell biology during infection with *Plasmodium* parasites.

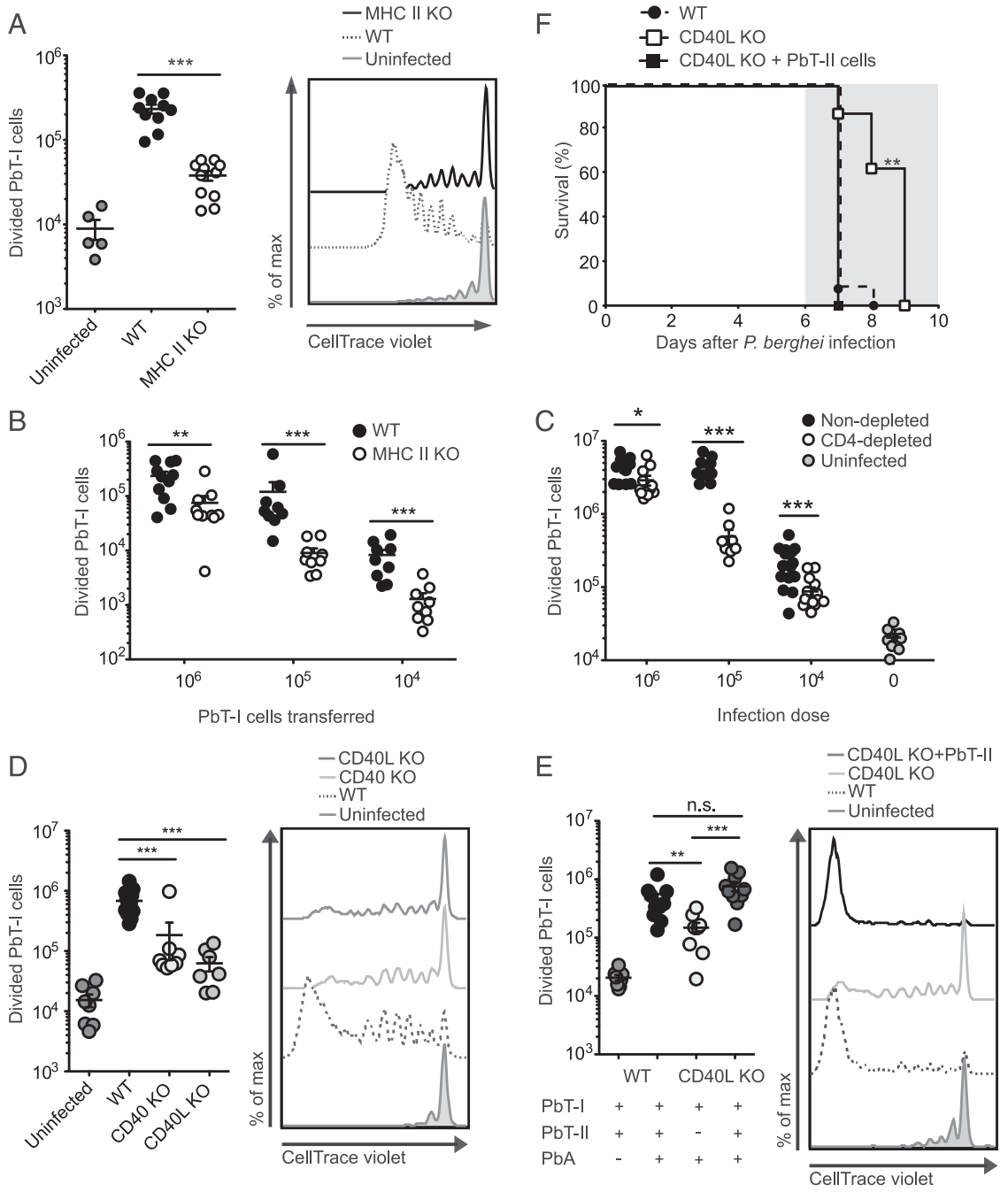

FIGURE 7. PbT-I priming during blood-stage PbA is enhanced by $CD4^+$ T cell help via CD40–CD40L interactions. (**A**) $CD4^+$ T cell help is required for PbT-I proliferation. CTV-labeled PbT-I/uGFP cells (10^6) were transferred into WT or MHC II–deficient (MHC II KO) mice 1 d before infection with 10^4 PbA iRBC. Numbers of divided PbT-I cells were assessed on day 5 postinfection. Left panel, Numbers of divided PbT-I cells in the spleen. Right panel, Representative histograms showing PbT-I cell division. (**B**) $CD4^+$ T cell help is required independently of the starting number of PbT-I cells. CTV-labeled PbT-I/uGFP cells (10^6, 10^5, or 10^4) were transferred into WT (filled circles) or MHC II–deficient (open circles) mice, which were infected with 10^4 PbA iRBC 1 d later. Numbers of divided PbT-I cells in the spleens were assessed on day 5 postinfection. (**C**) B6 mice were depleted of CD4 T cells by the injection of 100 μg of GK1.5 Ab on days −7 and −4 postinfection or left untreated and received 10^6 PbT-I cells 1 d before infection with 10^6, 10^5, or 10^4 PbA iRBC. Numbers of divided PbT-I cells were estimated on day 5 postinfection. Gray indicates PbT-I numbers in uninfected WT mice. Data were log transformed and analyzed using an unpaired *t* test. $*p < 0.05$, $**p < 0.01$, $***p < 0.001$. (**D**) PbT-I proliferation after PbA infection is decreased in CD40L-deficient (CD40L KO) and CD40-deficient (CD40 KO) mice. WT, CD40-deficient, or CD40L-deficient mice received 10^6 CTV-labeled PbT-I/uGFP cells and were infected with 10^4 PbA iRBC 1 d later. Numbers of divided PbT-I cells were assessed on day 5 postinfection. Left panel, Numbers of divided PbT-I cells in the spleen. Right panel, Representative histograms showing PbT-I cell division. (**E**) PbT-II cells restored PbT-I proliferation in PbA-infected CD40L-deficient mice. WT or CD40L-deficient mice were adoptively transferred with 10^6 CTV-labeled PbT-I cells, and some mice also received 10^6 CTV-labeled PbT-II cells. One day later, mice were infected with 10^4 PbA iRBC. Numbers of divided PbT-I cells were assessed on day 5 postinfection. Left panel, Numbers of divided PbT-I cells in the spleen. Right panel, Representative histograms showing PbT-I cell division. Data were log transformed and analyzed using one-way ANOVA and a Tukey multiple comparison test. $*p < 0.05$, $**p < 0.01$, $***p < 0.001$; n.s., not significant. In (A)–(E), data were pooled from two to four independent experiments and each point represents an individual mouse. (**F**) PbT-II cells accelerate ECM development in CD40L-deficient mice. CD40L-deficient mice received 10^6 PbT-II cells (filled squares, solid line) or no cells (open squares, solid line) and, together with WT control mice (filled circles, dotted line), were infected with 10^4 PbA iRBC 1 d later. Mice were then monitored for development (*Figure legend continues*)

The specific Ag recognized by PbT-II cells is yet to be defined. The broad cross-reactivity to different *Plasmodium* species suggests that the target epitope belongs to a conserved protein, likely to have an essential function in blood-stage parasites. The PbT-II target protein is also expressed during the pre-erythrocytic stage, as PbT-II cells also responded to RAS. It is possible that this protein is only expressed late during the liver stage, shortly before merozoites are released to the blood (80), allowing for a small window of Ag presentation during the liver stage of the parasite. However, the limited development of RAS within hepatocytes argues against this possibility. Alternatively, the abundance of this protein during the liver stage of the parasite cycle may be lower than during the blood stage. Further studies will be required to determine the exact Ag recognized by PbT-II cells.

DC are extremely efficient at initiating T cell responses in numerous infection models. We have been able to demonstrate a pivotal role for the $CD8^+$ DC subset in the priming of both $CD4^+$ and $CD8^+$ T cells during blood-stage PbA infection. Our results on $CD8^+$ T cell activation confirm previous ex vivo data showing a superior efficiency of $CD8^+$ DC at priming OT-I cells after exposure to transgenic PbA parasites expressing SIINFEKL (9). They are also consistent with in vivo studies showing a reduced number of activated endogenous $CD8^+$ T cells after PbA infection of mice deficient in $CD8^+$ DC (37, 38, 69). As $CD8^+$ DC possess specialized machinery for cross-presentation (34), this likely underlies their unique capacity to prime $CD8^+$ T cells during infection by *Plasmodium* species.

$CD8^+$ DC were also the main subset that stimulated D78 and PbT-II cells. To estimate the net contribution of the different DC subsets to MHC II presentation, the results obtained for D78 stimulation ex vivo (Fig. 5B), which show that $CD8^+$ DC are ~10-fold better than $CD4^+$ DC or DN DC at presentation, were adjusted to reflect the distinct abundance of sorted DC subsets in the spleen ($CD4^+$ DC, 55.1%; $CD8^+$ DC, 17.7%; DN DC, 13.4% of splenic $CD11c^{hi}$MHC II^{hi} cells). From this adjustment, we estimated that the contribution of $CD8^+$ DC to Ag presentation via MHC II was 67% of the total, whereas $CD4^+$ DC contributed 20%, and DN DC contributed the remaining 13% (with the combined $CD8^-$ DC subsets therefore contributing 33% of the total Ag presentation in the spleen). For this analysis, we chose to use DC activity ex vivo (Fig. 5B) over in vitro (Fig. 5A) because DN DC, which contain some immature $CD8^+$ DC (66), may have been able to mature during in vitro culture and capture increased amounts of available Ag (note higher hybridoma responses to DN DC in Fig. 5A than in Fig. 5B). In vivo experiments using different mouse lines deficient in $CD8^+$ DC to assess the contribution of $CD8^+$ DC to PbT-II priming during blood-stage PbA infection supported our observations with the D78 hybridoma: the number of dividing PbT-II cells in the spleen of Batf3-deficient, IRF8-deficient, or DT-treated XCR1-DTRvenus mice was reduced to 45.1, 16.6, and 31.0%, respectively. Because of the limitations of Batf3-deficient and IRF8-deficient mice in this system, with Batf3-deficient mice still containing immature DC capable of MHC II presentation (70, 71), and IRF8-deficient mice presenting additional immune defects (45, 72), the outcome using XCR1-DTRvenus mice (Fig. 6D, 6E) likely best represents the net contribution of $CD8^+$ DC to MHC II presentation. This value (69%) very closely aligns with the 67% contribution to MHC II presentation estimated using the D78 hybridoma.

These results clearly define $CD8^+$ DC as the major APC contributing to $CD4^+$ T cell priming during PbA infection. Previous work in our laboratory showed roughly equivalent $CD4^+$ T cell priming ex vivo by $CD8^-$ and $CD8^+$ DC from BALB/c mice infected with a transgenic PbA parasite expressing various model T cell epitopes (9). In that case, responses in B6 mice could not be assessed because they were too weak (9). Consistent with our present study, other reports have found an important role for $CD8^+$ DC in $CD4^+$ T cell activation: Clec9A-DTR mice depleted of $CD8^+$ DC by injection of DT showed a markedly decreased activation of endogenous $CD4^+$ T cells during PbA infection (37). Also, $CD8^+$ DC were more efficient than $CD8^-$ DC at presenting *P. chabaudi*–derived Ags to $CD4^+$ T cell hybridomas (39). In the latter study, the superiority of $CD8^+$ DC was only observed for DC derived from uninfected mice, and $CD8^-$ DC extracted on day 7 postinfection were more efficient at MHC II presentation than $CD8^+$ DC. At that late time point, $CD8^+$ DC showed greater cell death than $CD8^-$ DC, which likely explained their decreased stimulatory capacity (39). In vitro studies using model Ags showed a superior capacity for MHC II presentation by $CD8^-$ DC when the Ag used was either linked to beads or in a soluble form (34, 81). However, when presentation of cell-associated Ag was used, $CD8^+$ DC were superior (34). As blood-stage malaria Ags are largely cell associated, the superiority of $CD8^+$ DC in presenting MHC II–restricted malaria Ag shown in this study is likely a consequence of superiority in the capturing of malaria Ag. Indeed, a recent study has shown higher levels of *P. chabaudi* Ag uptake by $CD8^+$ DC relative to $CD4^+$ DC, when assessed at day 5 of infection (82).

We also provided evidence that $CD8^+$ DC contribute to the quality of the $CD4^+$ T cell response, as $CD8^+$ DC depletion led to the generation of reduced frequencies of Th1 and Tfh cells. This agrees with existing literature showing that the $CD8^+$ DC subset preferentially generates Th1 responses over Th2 responses (35, 36) and is efficient at promoting Tfh cell immunity (73, 74). The consequences of this functional capacity for $CD8^+$ DC, however, are likely to differ depending on the model studied, resulting in the induction of pathology or immunity. During PbA infection, for example, IFN-γ–producing $CD4^+$ T cells have been implicated in ECM by attracting $CD8^+$ T cells to the brain (83). Thus, $CD8^+$ DC may not only be crucial for initiation of $CD8^+$ T cell responses leading to ECM, but also for promoting Th1 cell development that in turn facilitates IFN-γ–dependent $CD8^+$ T cell recruitment to this organ. Alternatively, control of *P. chabaudi* infection largely requires Th1 cells during the first peak of parasitemia (84) and Tfh cells for complete elimination of the parasite (85). Tfh cells secrete several cytokines, such as IFN-γ, IL-2, IL-4, and IL-21. IL-2–, IL-4–, and IFN-γ–deficient mice experience more exacerbated relapses of parasitemia than do WT mice, but are eventually able to control the infection (86, 87). However, IL-21 KO mice are unable to control *P. chabaudi* parasitemia (88). Not surprisingly, the absence of $CD8^+$ DC in this infection results in impaired parasite control and more pronounced relapses (40).

The reason for the observed dominance of $CD8^+$ DC in MHC II presentation remains unclear. The form of Ag encountered by DC appears to play a role, as in the present work $CD8^+$ DC only outperformed other DC subsets when Ag was provided in a RBC-associated form, but not when in soluble form (Fig. 5C, 5D). This

of ECM. Survival curves of CD40L-deficient mice with or without PbT-II cells were statistically compared using a log-rank test. $^{**}p = 0.0011$. Data were pooled from two independent experiments including a total of 13 WT, 7 CD40L-deficient mice that received PbT-II cells, and 8 CD40L-deficient mice that did not receive PbT-II cells.

is consistent with their specialization in the capture of cell-associated Ag (89). Further studies are required to elucidate the mechanisms underlying the superiority of $CD8^+$ DC in MHC II presentation during PbA infection.

Transfer of WT PbT-II cells into CD40L KO mice sufficed to restore Ab production in these mice for efficient protection against *P. chabaudi* infection, highlighting the capacity of PbT-II cells, presumably of the Tfh cell subtype, to liaise with B cells for Ab production (90, 91). However, a beneficial effect of PbT-II cells was also observed in adoptively transferred RAG KO mice, which lack B cells. These mice survived longer than nontransferred RAG KO controls and displayed a lower primary peak of parasitemia (Fig. 4A, 4B, Supplemental Fig. 2A). A similar effect has been observed before after adoptive transfer of B5 cells into RAG KO mice subsequently infected with *P. chabaudi* (17) and has been linked to enhancement of parasite killing by CD4 T cell–derived IFN-γ or TNF-α (92).

Given the critical role of $CD8^+$ T cells in the development of ECM (93), determining the requirements for $CD8^+$ T cell activation during blood-stage malaria is of great importance. cDC are essential for the induction of ECM (68), and lack of ECM in XCR1-DTRvenus mice treated with DT early in infection confirms the findings of others (37) that implicate $CD8^+$ DC in this process. This is not surprising given their central role in priming both $CD4^+$ and $CD8^+$ T cells. Less clear is the extent to which $CD4^+$ T cell licensing of $CD8^+$ DC is required for ECM development. Several studies have shown that anti-$CD4^+$ Ab given around the time of PbA infection prevents ECM (26–30), consistent with the view that $CD4^+$ T cell help is required for the induction of CTL responses. However, $CD4^+$ T cells have also been implicated in $CD8^+$ T cell recruitment to the brain (83), thus raising the possibility that their depletion merely affects this facet of disease. Only one study provides direct evidence for a contribution of $CD4^+$ T cell help to $CD8^+$ T cell proliferation, where $CD4^+$ T cell depletion resulted in low proliferation of OVA-specific OT-I cells after infection with transgenic PbA parasites expressing the OVA epitope (31). By using our PbT-I transgenic $CD8^+$ T cells, we clearly demonstrated that $CD4^+$ T cell help was essential for optimal $CD8^+$ T cell expansion, as mice depleted of $CD4^+$ T cells showed suboptimal PbT-I proliferation. These responses were dependent on $CD8^+$ DC, as they were impaired when this subset of DC was depleted. Furthermore, they depended heavily on CD40L, as mice deficient in this molecule had curtailed $CD8^+$ T cell proliferation. The capacity of transferred PbT-II cells to help PbT-I cells to proliferate in CD40L-deficient mice further implicated CD40L as an important component of help that could be provided by PbT-II T cells. Interestingly, CD40 signaling was not absolutely essential for ECM development, as CD40L-deficient mice eventually developed ECM in the absence of added PbT-II T cells, although with a delayed kinetics. This contrasts a previous report that found CD40L-deficient mice were resistant to ECM (94), an observation that may be explained by differences in animal housing facilities, potentially microbiota, known to affect ECM (95). In summary, our work extends earlier findings by determining that $CD4^+$ T cell help is required for optimal $CD8^+$ T cell expansion after infection with different doses of parasites, and is relatively independent of the initial $CD8^+$ T cell precursor frequency. By defining CD40 signaling as an important event in DC licensing in this model, we have also identified a key checkpoint that could be targeted to limit pathogenic $CD8^+$ T cell immunity to blood-stage disease.

We have established that $CD8^+$ DC are the main APC for $CD4^+$ and $CD8^+$ T cell priming, and that $CD8^+$ T cell priming required $CD4^+$ T cell help. It is likely that $CD8^+$ DC are licensed by those $CD4^+$ T cells that they prime, although $CD4^+$ T cells primed on $CD8^-$ DC may also contribute to this process. The essential role for $CD8^+$ DC in $CD8^+$ T cell priming and their dominant role in $CD4^+$ T cell priming puts this subset at the center of response initiation to blood-stage malaria parasites and suggests that strategies aimed at generating T cell responses against blood-stage malaria parasites will benefit from exploiting this DC subtype. The findings that individuals with severe disease in malaria endemic areas present with increased numbers of circulating $BDCA3^+$ DC (96) (the human equivalent to mouse $CD8^+$ DC) and activated $CD8^+$ T cells (38) relative to those with mild malaria suggest that $CD8^+$ T cell activation during blood-stage malaria may be driven by a similar process in humans as in the mouse model. More precise knowledge of the mechanisms that drive $CD8^+$ DC function during malarial infections may thus allow us to develop more effective strategies to combat this disease.

Acknowledgments

We thank Melanie Damtsis and Ming Li for technical assistance, and members of the F.R.C. and W.R.H. laboratories for discussion and the staff of The Peter Doherty Institute animal facility for animal husbandry. We thank the Melbourne Brain Centre and ImmunoID Flow Cytometry Facility for technical assistance.

Disclosures

The authors have no financial conflicts of interest.

References

1. World Health Organization. 2015. World Malaria Report 2015. Geneva, Switzerland: World Health Organization.Available at: http://www.who.int/malaria/publications/world-malaria-report-2015/report/en/.
2. Carvalho, L. H., G.-i. Sano, J. C. R. Hafalla, A. Morrot, M. A. Curotto de Lafaille, and F. Zavala. 2002. IL-4-secreting $CD4^+$ T cells are crucial to the development of $CD8^+$ T-cell responses against malaria liver stages. *Nat. Med.* 8: 166–170.
3. Krishnegowda, G., A. M. Hajjar, J. Zhu, E. J. Douglass, S. Uematsu, S. Akira, A. S. Woods, and D. C. Gowda. 2005. Induction of proinflammatory responses in macrophages by the glycosylphosphatidylinositols of *Plasmodium falciparum*: cell signaling receptors, glycosylphosphatidylinositol (GPI) structural requirement, and regulation of GPI activity. *J. Biol. Chem.* 280: 8606–8616.
4. Overstreet, M. G., Y.-C. Chen, I. A. Cockburn, S.-W. Tse, and F. Zavala. 2011. $CD4^+$ T cells modulate expansion and survival but not functional properties of effector and memory $CD8^+$ T cells induced by malaria sporozoites. *PLoS One* 6: e15948.
5. Craig, A. G., G. E. Grau, C. Janse, J. W. Kazura, D. Milner, J. W. Barnwell, G. Turner, and J. Langhorne, participants of the Hinxton Retreat meeting on Animal Models for Research on Severe Malaria. 2012. The role of animal models for research on severe malaria. *PLoS Pathog.* 8: e1002401.
6. González-Aseguinolaza, G., C. de Oliveira, M. Tomaska, S. Hong, O. Bruña-Romero, T. Nakayama, M. Taniguchi, A. Bendelac, L. Van Kaer, Y. Koezuka, and M. Tsuji. 2000. α-Galactosylceramide-activated Vα14 natural killer T cells mediate protection against murine malaria. *Proc. Natl. Acad. Sci. USA* 97: 8461–8466.
7. Coban, C., K. J. Ishii, T. Kawai, H. Hemmi, S. Sato, S. Uematsu, M. Yamamoto, O. Takeuchi, S. Itagaki, N. Kumar, et al. 2005. Toll-like receptor 9 mediates innate immune activation by the malaria pigment hemozoin. *J. Exp. Med.* 201: 19–25.
8. Romero, J. F., G. Eberl, H. R. MacDonald, and G. Corradin. 2001. CD1d-restricted NK T cells are dispensable for specific antibody responses and protective immunity against liver stage malaria infection in mice. *Parasite Immunol.* 23: 267–269.
9. Lundie, R. J., T. F. de Koning-Ward, G. M. Davey, C. Q. Nie, D. S. Hansen, L. S. Lau, J. D. Mintern, G. T. Belz, L. Schofield, F. R. Carbone, et al. 2008. Blood-stage *Plasmodium* infection induces $CD8^+$ T lymphocytes to parasite-expressed antigens, largely regulated by $CD8\alpha^+$ dendritic cells. *Proc. Natl. Acad. Sci. USA* 105: 14509–14514.
10. Miyakoda, M., D. Kimura, M. Yuda, Y. Chinzei, Y. Shibata, K. Honma, and K. Yui. 2008. Malaria-specific and nonspecific activation of $CD8^+$ T cells during blood stage of *Plasmodium berghei* infection. *J. Immunol.* 181: 1420–1428.
11. Korten, S., R. J. Anderson, C. M. Hannan, E. G. Sheu, R. Sinden, S. Gadola, M. Taniguchi, and A. V. S. Hill. 2005. Invariant Vα14 chain NKT cells promote *Plasmodium berghei* circumsporozoite protein-specific γ interferon- and tumor necrosis factor α-producing $CD8^+$ T cells in the liver after poxvirus vaccination of mice. *Infect. Immun.* 73: 849–858.
12. Lundie, R. J., L. J. Young, G. M. Davey, J. A. Villadangos, F. R. Carbone, W. R. Heath, and B. S. Crabb. 2010. Blood-stage *Plasmodium berghei* infection

leads to short-lived parasite-associated antigen presentation by dendritic cells. *Eur. J. Immunol.* 40: 1674–1681.
13. Haque, A., S. E. Best, K. Unosson, F. H. Amante, F. de Labastida, N. M. Anstey, G. Karupiah, M. J. Smyth, W. R. Heath, and C. R. Engwerda. 2011. Granzyme B expression by $CD8^+$ T cells is required for the development of experimental cerebral malaria. *J. Immunol.* 186: 6148–6156.
14. González-Aseguinolaza, G., L. Van Kaer, C. C. Bergmann, J. M. Wilson, J. Schmieg, M. Kronenberg, T. Nakayama, M. Taniguchi, Y. Koezuka, and M. Tsuji. 2002. Natural killer T cell ligand α-galactosylceramide enhances protective immunity induced by malaria vaccines. *J. Exp. Med.* 195: 617–624.
15. Miyakoda, M., D. Kimura, K. Honma, K. Kimura, M. Yuda, and K. Yui. 2012. Development of memory $CD8^+$ T cells and their recall responses during blood-stage infection with *Plasmodium berghei* ANKA. *J. Immunol.* 189: 4396–4404.
16. Lau, L. S., D. Fernández-Ruiz, V. Mollard, A. Sturm, M. A. Neller, A. Cozijnsen, J. L. Gregory, G. M. Davey, C. M. Jones, Y.-H. Lin, et al. 2014. $CD8^+$ T cells from a novel T cell receptor transgenic mouse induce liver-stage immunity that can be boosted by blood-stage infection in rodent malaria. *PLoS Pathog.* 10: e1004135.
17. Stephens, R., F. R. Albano, S. Quin, B. J. Pascal, V. Harrison, B. Stockinger, D. Kioussis, H.-U. Weltzien, and J. Langhorne. 2005. Malaria-specific transgenic $CD4^+$ T cells protect immunodeficient mice from lethal infection and demonstrate requirement for a protective threshold of antibody production for parasite clearance. *Blood* 106: 1676–1684.
18. Smith, C. M., N. S. Wilson, J. Waithman, J. A. Villadangos, F. R. Carbone, W. R. Heath, and G. T. Belz. 2004. Cognate $CD4^+$ T cell licensing of dendritic cells in $CD8^+$ T cell immunity. *Nat. Immunol.* 5: 1143–1148.
19. Belz, G. T., D. Wodarz, G. Diaz, M. A. Nowak, and P. C. Doherty. 2002. Compromised influenza virus-specific $CD8^+$-T-cell memory in $CD4^+$-T-cell-deficient mice. *J. Virol.* 76: 12388–12393.
20. Matloubian, M., R. J. Concepcion, and R. Ahmed. 1994. $CD4^+$ T cells are required to sustain $CD8^+$ cytotoxic T-cell responses during chronic viral infection. *J. Virol.* 68: 8056–8063.
21. Sun, J. C., and M. J. Bevan. 2003. Defective CD8 T cell memory following acute infection without CD4 T cell help. *Science* 300: 339–342.
22. Bachmann, M. F., R. M. Zinkernagel, and A. Oxenius. 1998. Immune responses in the absence of costimulation: viruses know the trick. *J. Immunol.* 161: 5791–5794.
23. Schmieg, J., G. González-Aseguinolaza, and M. Tsuji. 2003. The role of natural killer T cells and other T cell subsets against infection by the pre-erythrocytic stages of malaria parasites. *Microbes Infect.* 5: 499–506.
24. Le Bon, A., N. Etchart, C. Rossmann, M. Ashton, S. Hou, D. Gewert, P. Borrow, and D. F. Tough. 2003. Cross-priming of $CD8^+$ T cells stimulated by virus-induced type I interferon. *Nat. Immunol.* 4: 1009–1015.
25. Schofield, L., and G. E. Grau. 2005. Immunological processes in malaria pathogenesis. *Nat. Rev. Immunol.* 5: 722–735.
26. Grau, G. E., P. F. Piguet, H. D. Engers, J. A. Louis, P. Vassalli, and P. H. Lambert. 1986. $L3T4^+$ T lymphocytes play a major role in the pathogenesis of murine cerebral malaria. *J. Immunol.* 137: 2348–2354.
27. Yañez, D. M., D. D. Manning, A. J. Cooley, W. P. Weidanz, and H. C. van der Heyde. 1996. Participation of lymphocyte subpopulations in the pathogenesis of experimental murine cerebral malaria. *J. Immunol.* 157: 1620–1624.
28. Belnoue, E., M. Kayibanda, A. M. Vigário, J.-C. Deschemin, N. van Rooijen, M. Viguier, G. Snounou, and L. Rénia. 2002. On the pathogenic role of brain-sequestered αβ $CD8^+$ T cells in experimental cerebral malaria. *J. Immunol.* 169: 6369–6375.
29. Hermsen, C., T. van de Wiel, E. Mommers, R. Sauerwein, and W. Eling. 1997. Depletion of $CD4^+$ or $CD8^+$ T-cells prevents *Plasmodium berghei* induced cerebral malaria in end-stage disease. *Parasitology* 114: 7–12.
30. Waki, S., S. Uehara, K. Kanbe, K. Ono, M. Suzuki, and H. Nariuchi. 1992. The role of T cells in pathogenesis and protective immunity to murine malaria. *Immunology* 75: 646–651.
31. Haque, A., S. E. Best, A. Ammerdorffer, L. Desbarrieres, M. M. de Oca, F. H. Amante, F. de Labastida Rivera, P. Hertzog, G. M. Boyle, G. R. Hill, and C. R. Engwerda. 2011. Type I interferons suppress $CD4^+$ T-cell-dependent parasite control during blood-stage *Plasmodium* infection. *Eur. J. Immunol.* 41: 2688–2698.
32. Pulendran, B. 2015. The varieties of immunological experience: of pathogens, stress, and dendritic cells. *Annu. Rev. Immunol.* 33: 563–606.
33. den Haan, J. M., S. M. Lehar, and M. J. Bevan. 2000. $CD8^+$ but not $CD8^-$ dendritic cells cross-prime cytotoxic T cells in vivo. *J. Exp. Med.* 192: 1685–1696.
34. Schnorrer, P., G. M. N. Behrens, N. S. Wilson, J. L. Pooley, C. M. Smith, D. El-Sukkari, G. Davey, F. Kupresanin, M. Li, E. Maraskovsky, et al. 2006. The dominant role of $CD8^+$ dendritic cells in cross-presentation is not dictated by antigen capture. *Proc. Natl. Acad. Sci. USA* 103: 10729–10734.
35. Pulendran, B., J. L. Smith, G. Caspary, K. Brasel, D. Pettit, E. Maraskovsky, and C. R. Maliszewski. 1999. Distinct dendritic cell subsets differentially regulate the class of immune response in vivo. *Proc. Natl. Acad. Sci. USA* 96: 1036–1041.
36. Maldonado-López, R., T. De Smedt, P. Michel, J. Godfroid, B. Pajak, C. Heirman, K. Thielemans, O. Leo, J. Urbain, and M. Moser. 1999. $CD8\alpha^+$ and $CD8\alpha^-$ subclasses of dendritic cells direct the development of distinct T helper cells in vivo. *J. Exp. Med.* 189: 587–592.
37. Piva, L., P. Tetlak, C. Claser, K. Karjalainen, L. Renia, and C. Ruedl. 2012. Cutting edge: $Clec9A^+$ dendritic cells mediate the development of experimental cerebral malaria. *J. Immunol.* 189: 1128–1132.
38. Guermonprez, P., J. Helft, C. Claser, S. Deroubaix, H. Karanje, A. Gazumyan, G. Darasse-Jèze, S. B. Telerman, G. Breton, H. A. Schreiber, et al. 2013. Inflammatory Flt3l is essential to mobilize dendritic cells and for T cell responses during *Plasmodium* infection. *Nat. Med.* 19: 730–738.
39. Sponaas, A.-M., E. T. Cadman, C. Voisine, V. Harrison, A. Boonstra, A. O'Garra, and J. Langhorne. 2006. Malaria infection changes the ability of splenic dendritic cell populations to stimulate antigen-specific T cells. *J. Exp. Med.* 203: 1427–1433.
40. Turcotte, K., S. Gauthier, D. Malo, M. Tam, M. M. Stevenson, and P. Gros. 2007. *Icsbp1*/IRF-8 is required for innate and adaptive immune responses against intracellular pathogens. *J. Immunol.* 179: 2467–2476.
41. Vugmeyster, Y., R. Glas, B. Pérarnau, F. A. Lemonnier, H. Eisen, and H. Ploegh. 1998. Major histocompatibility complex (MHC) class I $K^bD^{b\,-/-}$ deficient mice possess functional $CD8^+$ T cells and natural killer cells. *Proc. Natl. Acad. Sci. USA* 95: 12492–12497.
42. Madsen, L., N. Labrecque, J. Engberg, A. Dierich, A. Svejgaard, C. Benoist, D. Mathis, and L. Fugger. 1999. Mice lacking all conventional MHC class II genes. *Proc. Natl. Acad. Sci. USA* 96: 10338–10343.
43. Mombaerts, P., J. Iacomini, R. S. Johnson, K. Herrup, S. Tonegawa, and V. E. Papaioannou. 1992. RAG-1-deficient mice have no mature B and T lymphocytes. *Cell* 68: 869–877.
44. Hildner, K., B. T. Edelson, W. E. Purtha, M. Diamond, H. Matsushita, M. Kohyama, B. Calderon, B. U. Schraml, E. R. Unanue, M. S. Diamond, et al. 2008. Batf3 deficiency reveals a critical role for $CD8\alpha^+$ dendritic cells in cytotoxic T cell immunity. *Science* 322: 1097–1100.
45. Holtschke, T., J. Löhler, Y. Kanno, T. Fehr, N. Giese, F. Rosenbauer, J. Lou, K. P. Knobeloch, L. Gabriele, J. F. Waring, et al. 1996. Immunodeficiency and chronic myelogenous leukemia-like syndrome in mice with a targeted mutation of the ICSBP gene. *Cell* 87: 307–317.
46. Yamazaki, C., M. Sugiyama, T. Ohta, H. Hemmi, E. Hamada, I. Sasaki, Y. Fukuda, T. Yano, M. Nobuoka, T. Hirashima, et al. 2013. Critical roles of a dendritic cell subset expressing a chemokine receptor, XCR1. *J. Immunol.* 190: 6071–6082.
47. Jung, S., D. Unutmaz, P. Wong, G. Sano, K. De los Santos, T. Sparwasser, S. Wu, S. Vuthoori, K. Ko, F. Zavala, et al. 2002. *In vivo* depletion of $CD11c^+$ dendritic cells abrogates priming of $CD8^+$ T cells by exogenous cell-associated antigens. *Immunity* 17: 211–220.
48. Kawabe, T., T. Naka, K. Yoshida, T. Tanaka, H. Fujiwara, S. Suematsu, N. Yoshida, T. Kishimoto, and H. Kikutani. 1994. The immune responses in CD40-deficient mice: impaired immunoglobulin class switching and germinal center formation. *Immunity* 1: 167–178.
49. Xu, J., T. M. Foy, J. D. Laman, E. A. Elliott, J. J. Dunn, T. J. Waldschmidt, J. Elsemore, R. J. Noelle, and R. A. Flavell. 1994. Mice deficient for the CD40 ligand. *Immunity* 1: 423–431.
50. Barnden, M. J., J. Allison, W. R. Heath, and F. R. Carbone. 1998. Defective TCR expression in transgenic mice constructed using cDNA-based α- and β-chain genes under the control of heterologous regulatory elements. *Immunol. Cell Biol.* 76: 34–40.
51. Bedoui, S., P. G. Whitney, J. Waithman, L. Eidsmo, L. Wakim, I. Caminschi, R. S. Allan, M. Wojtasiak, K. Shortman, F. R. Carbone, et al. 2009. Cross-presentation of viral and self antigens by skin-derived $CD103^+$ dendritic cells. *Nat. Immunol.* 10: 488–495.
52. Benedict, M. Q. 1997. Care and maintenance of anopheline mosquito colonies. In *The Molecular Biology of Insect Disease Vectors*. J. M. Crampton, and C. B. Beard, and C. Louis, eds. Springer, Dordrecht, the Netherlands, p. 3–12
53. Trager, W., and J. B. Jensen. 1976. Human malaria parasites in continuous culture. *Science* 193: 673–675.
54. Lau, L. S., D. Fernandez Ruiz, G. M. Davey, T. F. de Koning-Ward, A. T. Papenfuss, F. R. Carbone, A. G. Brooks, B. S. Crabb, and W. R. Heath. 2011. Blood-stage *Plasmodium berghei* infection generates a potent, specific $CD8^+$ T-cell response despite residence largely in cells lacking MHC I processing machinery. *J. Infect. Dis.* 204: 1989–1996.
55. Mueller, S. N., C. M. Jones, C. M. Smith, W. R. Heath, and F. R. Carbone. 2002. Rapid cytotoxic T lymphocyte activation occurs in the draining lymph nodes after cutaneous herpes simplex virus infection as a result of early antigen presentation and not the presence of virus. *J. Exp. Med.* 195: 651–656.
56. Kaye, J., N. J. Vasquez, and S. M. Hedrick. 1992. Involvement of the same region of the T cell antigen receptor in thymic selection and foreign peptide recognition. *J. Immunol.* 148: 3342–3353.
57. Smith, C. M., G. T. Belz, N. S. Wilson, J. A. Villadangos, K. Shortman, F. R. Carbone, and W. R. Heath. 2003. Cutting edge: conventional $CD8\alpha^+$ dendritic cells are preferentially involved in CTL priming after footpad infection with herpes simplex virus-1. *J. Immunol.* 170: 4437–4440.
58. Sanderson, S., and N. Shastri. 1994. LacZ inducible, antigen/MHC-specific T cell hybrids. *Int. Immunol.* 6: 369–376.
59. Clarke, S. R., M. Barnden, C. Kurts, F. R. Carbone, J. F. Miller, and W. R. Heath. 2000. Characterization of the ovalbumin-specific TCR transgenic line OT-I: MHC elements for positive and negative selection. *Immunol. Cell Biol.* 78: 110–117.
60. Heath, W. R., and J. F. Miller. 1993. Expression of two alpha chains on the surface of T cells in T cell receptor transgenic mice. *J. Exp. Med.* 178: 1807–1811.
61. Langhorne, J., B. Simon-Haarhaus, and S. J. Meding. 1990. The role of $CD4^+$ T cells in the protective immune response to *Plasmodium chabaudi* in vivo. *Immunol. Lett.* 25: 101–107.
62. Meding, S. J., and J. Langhorne. 1991. $CD4^+$ T cells and B cells are necessary for the transfer of protective immunity to *Plasmodium chabaudi chabaudi. Eur. J. Immunol.* 21: 1433–1438.

63. Voisine, C., B. Mastelic, A.-M. Sponaas, and J. Langhorne. 2010. Classical CD11c$^+$ dendritic cells, not plasmacytoid dendritic cells, induce T cell responses to *Plasmodium chabaudi* malaria. *Int. J. Parasitol.* 40: 711–719.
64. Vremec, D., J. Pooley, H. Hochrein, L. Wu, and K. Shortman. 2000. CD4 and CD8 expression by dendritic cell subtypes in mouse thymus and spleen. *J. Immunol.* 164: 2978–2986.
65. Caminschi, I., A. I. Proietto, F. Ahmet, S. Kitsoulis, J. Shin Teh, J. C. Y. Lo, A. Rizzitelli, L. Wu, D. Vremec, S. L. H. van Dommelen, et al. 2008. The dendritic cell subtype-restricted C-type lectin Clec9A is a target for vaccine enhancement. *Blood* 112: 3264–3273.
66. Naik, S. H., D. Metcalf, A. van Nieuwenhuijze, I. Wicks, L. Wu, M. O'Keeffe, and K. Shortman. 2006. Intrasplenic steady-state dendritic cell precursors that are distinct from monocytes. *Nat. Immunol.* 7: 663–671.
67. Mintern, J. D., C. Macri, and J. A. Villadangos. 2015. Modulation of antigen presentation by intracellular trafficking. *Curr. Opin. Immunol.* 34: 16–21.
68. deWalick, S., F. H. Amante, K. A. McSweeney, L. M. Randall, A. C. Stanley, A. Haque, R. D. Kuns, K. P. A. MacDonald, G. R. Hill, and C. R. Engwerda. 2007. Cutting edge: conventional dendritic cells are the critical APC required for the induction of experimental cerebral malaria. *J. Immunol.* 178: 6033–6037.
69. Zhao, H., T. Aoshi, S. Kawai, Y. Mori, A. Konishi, M. Ozkan, Y. Fujita, Y. Haseda, M. Shimizu, M. Kohyama, et al. 2014. Olfactory plays a key role in spatiotemporal pathogenesis of cerebral malaria. *Cell Host Microbe* 15: 551–563.
70. Edelson, B. T., T. R. Bradstreet, W. Kc, K. Hildner, J. W. Herzog, J. Sim, J. H. Russell, T. L. Murphy, E. R. Unanue, and K. M. Murphy. 2011. Batf3-dependent CD11b$^{low/-}$ peripheral dendritic cells are GM-CSF-independent and are not required for Th cell priming after subcutaneous immunization. *PLoS One* 6: e25660.
71. Caminschi, I., D. Vremec, F. Ahmet, M. H. Lahoud, J. A. Villadangos, K. M. Murphy, W. R. Heath, and K. Shortman. 2012. Antibody responses initiated by Clec9A-bearing dendritic cells in normal and Batf3$^{-/-}$ mice. *Mol. Immunol.* 50: 9–17.
72. Aliberti, J., O. Schulz, D. J. Pennington, H. Tsujimura, C. Reis e Sousa, K. Ozato, and A. Sher. 2003. Essential role for ICSBP in the in vivo development of murine CD8α^+ dendritic cells. *Blood* 101: 305–310.
73. Kato, Y., A. Zaid, G. M. Davey, S. N. Mueller, S. L. Nutt, D. Zotos, D. M. Tarlinton, K. Shortman, M. H. Lahoud, W. R. Heath, and I. Caminschi. 2015. Targeting antigen to Clec9A primes follicular Th cell memory responses capable of robust recall. *J. Immunol.* 195: 1006–1014.
74. Lahoud, M. H., F. Ahmet, S. Kitsoulis, S. S. Wan, D. Vremec, C. N. Lee, B. Phipson, W. Shi, G. K. Smyth, A. M. Lew, et al. 2011. Targeting antigen to mouse dendritic cells via Clec9A induces potent CD4 T cell responses biased toward a follicular helper phenotype. *J. Immunol.* 187: 842–850.
75. Iborra, S., M. Martínez-López, S. C. Khouili, M. Enamorado, F. J. Cueto, R. Conde-Garrosa, C. Del Fresno, and D. Sancho. 2016. Optimal generation of tissue-resident but not circulating memory T cells during viral infection requires crosspriming by DNGR-1$^+$ dendritic cells. *Immunity* 45: 847–860.
76. Mintern, J. D., G. M. Davey, G. T. Belz, F. R. Carbone, and W. R. Heath. 2002. Cutting edge: precursor frequency affects the helper dependence of cytotoxic T cells. *J. Immunol.* 168: 977–980.
77. Bennett, S. R., F. R. Carbone, F. Karamalis, R. A. Flavell, J. F. Miller, and W. R. Heath. 1998. Help for cytotoxic-T-cell responses is mediated by CD40 signalling. *Nature* 393: 478–480.
78. Ridge, J. P., F. Di Rosa, and P. Matzinger. 1998. A conditioned dendritic cell can be a temporal bridge between a CD4$^+$ T-helper and a T-killer cell. *Nature* 393: 474–478.
79. Schoenberger, S. P., R. E. Toes, E. I. van der Voort, R. Offringa, and C. J. Melief. 1998. T-cell help for cytotoxic T lymphocytes is mediated by CD40–CD40L interactions. *Nature* 393: 480–483.
80. Sturm, A., R. Amino, C. van de Sand, T. Regen, S. Retzlaff, A. Rennenberg, A. Krueger, J. M. Pollok, R. Menard, and V. T. Heussler. 2006. Manipulation of host hepatocytes by the malaria parasite for delivery into liver sinusoids. *Science* 313: 1287–1290.
81. Kamphorst, A. O., P. Guermonprez, D. Dudziak, and M. C. Nussenzweig. 2010. Route of antigen uptake differentially impacts presentation by dendritic cells and activated monocytes. *J. Immunol.* 185: 3426–3435.
82. Borges da Silva, H., R. Fonseca, A. A. Cassado, É. Machado de Salles, M. N. de Menezes, J. Langhorne, K. R. Perez, I. M. Cuccovia, B. Ryffel, V. M. Barreto, et al. 2015. In vivo approaches reveal a key role for DCs in CD4$^+$ T cell activation and parasite clearance during the acute phase of experimental blood-stage malaria. *PLoS Pathog.* 11: e1004598.
83. Villegas-Mendez, A., R. Greig, T. N. Shaw, J. B. de Souza, E. Gwyer Findlay, J. S. Stumhofer, J. C. R. Hafalla, D. G. Blount, C. A. Hunter, E. M. Riley, and K. N. Couper. 2012. IFN-γ–producing CD4$^+$ T cells promote experimental cerebral malaria by modulating CD8$^+$ T cell accumulation within the brain. *J. Immunol.* 189: 968–979.
84. Su, Z., and M. M. Stevenson. 2002. IL-12 is required for antibody-mediated protective immunity against blood-stage *Plasmodium chabaudi* AS malaria infection in mice. *J. Immunol.* 168: 1348–1355.
85. Wikenheiser, D. J., D. Ghosh, B. Kennedy, and J. S. Stumhofer. 2016. The costimulatory molecule ICOS regulates host Th1 and follicular Th cell differentiation in response to *Plasmodium chabaudi chabaudi* AS infection. *J. Immunol.* 196: 778–791.
86. van der Heyde, H. C., B. Pepper, J. Batchelder, F. Cigel, and W. P. Weidanz. 1997. The time course of selected malarial infections in cytokine-deficient mice. *Exp. Parasitol.* 85: 206–213.
87. von der Weid, T., M. Kopf, G. Köhler, and J. Langhorne. 1994. The immune response to *Plasmodium chabaudi* malaria in interleukin-4-deficient mice. *Eur. J. Immunol.* 24: 2285–2293.
88. Pérez-Mazliah, D., D. H. L. Ng, A. P. Freitas do Rosário, S. McLaughlin, B. Mastelic-Gavillet, J. Sodenkamp, G. Kushinga, and J. Langhorne. 2015. Disruption of IL-21 signaling affects T cell-B cell interactions and abrogates protective humoral immunity to malaria. *PLoS Pathog.* 11: e1004715.
89. Iyoda, T., S. Shimoyama, K. Liu, Y. Omatsu, Y. Akiyama, Y. Maeda, K. Takahara, R. M. Steinman, and K. Inaba. 2002. The CD8$^+$ dendritic cell subset selectively endocytoses dying cells in culture and in vivo. *J. Exp. Med.* 195: 1289–1302.
90. Schaerli, P., K. Willimann, A. B. Lang, M. Lipp, P. Loetscher, and B. Moser. 2000. CXC chemokine receptor 5 expression defines follicular homing T cells with B cell helper function. *J. Exp. Med.* 192: 1553–1562.
91. Breitfeld, D., L. Ohl, E. Kremmer, J. Ellwart, F. Sallusto, M. Lipp, and R. Förster. 2000. Follicular B helper T cells express CXC chemokine receptor 5, localize to B cell follicles, and support immunoglobulin production. *J. Exp. Med.* 192: 1545–1552.
92. Stephens, R., and J. Langhorne. 2010. Effector memory Th1 CD4 T cells are maintained in a mouse model of chronic malaria. *PLoS Pathog.* 6: e1001208.
93. Nitcheu, J., O. Bonduelle, C. Combadiere, M. Tefit, D. Seilhean, D. Mazier, and B. Combadiere. 2003. Perforin-dependent brain-infiltrating cytotoxic CD8$^+$ T lymphocytes mediate experimental cerebral malaria pathogenesis. *J. Immunol.* 170: 2221–2228.
94. Piguet, P. F., C. D. Kan, C. Vesin, A. Rochat, Y. Donati, and C. Barazzone. 2001. Role of CD40-CVD40L in mouse severe malaria. *Am. J. Pathol.* 159: 733–742.
95. Villarino, N. F., G. R. LeCleir, J. E. Denny, S. P. Dearth, C. L. Harding, S. S. Sloan, J. L. Gribble, S. R. Campagna, S. W. Wilhelm, and N. W. Schmidt. 2016. Composition of the gut microbiota modulates the severity of malaria. *Proc. Natl. Acad. Sci. USA* 113: 2235–2240.
96. Urban, B. C., D. Cordery, M. J. Shafi, P. C. Bull, C. I. Newbold, T. N. Williams, and K. Marsh. 2006. The frequency of BDCA3-positive dendritic cells is increased in the peripheral circulation of Kenyan children with severe malaria. *Infect. Immun.* 74: 6700–6706.